Journal of Inflammation Research

Dovepress
Taylor & Francis Group

Open Access Full Text Article

ORIGINAL RESEARCH

Exploring *Salvia miltiorrhiza*'s Therapeutic Effects on Adenomyosis by Inhibiting TNF-α/HIF-1α/IL-17-Driven Inflammatory Cascade: Mechanistic Insights from Target Prediction and Experimental Validation

Qiaomei Yang[1,*], Jingxuan Hong[2,3,*], Xinye Zheng[1,*], Xianhua Liu[4], Hao Lin[1], Li Chen[1], Fuchun Zhong[5], Qianhui Zhang[1], Junying Jiang[1], PengMing Sun[1]

[1]Department of Gynecology, Fujian Maternity and Child Health Hospital, College of Clinical Medicine for Obstetrics & Gynecology and Pediatrics, Fujian Medical University, Fuzhou, Fujian, 350001, People's Republic of China; [2]Department of Cardiology, Fujian Provincial Hospital, Provincial Hospital Affiliated to Fuzhou University, Fuzhou, Fujian, 350001, People's Republic of China; [3]Department of Cardiology, Provincial Clinical Medical College of Fujian Medical University, Fuzhou, Fujian, 350001, People's Republic of China; [4]Department of Pathology, Fujian Maternity and Child Health Hospital College of Clinical Medicine for Obstetrics & Gynecology and Pediatrics, Fujian Medical University, Fuzhou, Fujian, 350001, People's Republic of China; [5]Department of Laboratory Medicine, Fujian Maternity and Child Health Hospital Affiliated to Fujian Medical University, Fuzhou, Fujian, 350001, People's Republic of China

*These authors contributed equally to this work

Correspondence: Junying Jiang; PengMing Sun, Email jiangjyf53@163.com; fmsun1975@fjmu.edu.cn

Background: Adenomyosis is a chronic inflammatory gynecological disorder closely linked with diminished fertility potential that poses significant challenges in pharmacological management. *Salvia miltiorrhiza* (Danshen, DS), a traditional Chinese herb with proven anti-inflammatory properties, has shown efficacy in treating chronic inflammatory conditions across multiple organ systems. However, its mechanisms in addressing adenomyosis remain unclear.

Methods: Ultra-performance liquid chromatography coupled with Q Exactive™ HF-X mass spectrometry (UPLC-QE-MS) was employed to identify the constituents of DS. Targets for DS in treating adenomyosis were identified from various databases and a PPI network was constructed. Core target genes were identified by Module analysis using MCODE and CytoNCA plugin of Cytoscape. Functional analyses of core target genes were performed using GO and KEGG, followed by molecular docking, transcriptomics validation, and molecular dynamics simulations. Predicted targets and pathways were validated through Western blotting, qRT-PCR, and IF.

Results: Thirty-five potential bioactive components from ingredients absorbed into the bloodstream (IAIBs) of DS were identified. Network pharmacology predicted that DS might exert therapeutic effects on adenomyosis by modulating the TNF-α/IL-17/HIF-1α signaling pathways through key targets, including *TNF, IL1β, MMP2, ESR1, PTGS2, STAT3, BCL2, AKT1, MMP9, and EGFR*. Molecular docking demonstrated that the active components have strong affinities with these core targets. Transcriptomic profiling identified *TNF* and *IL-1β* as key therapeutic targets in DS-adenomyosis. Molecular dynamics simulations exhibited that the active components form stable conformations with the inflammation-related therapeutic targets TNF and IL-1β. In vivo showed that DS significantly improved pathological changes in adenomyosis mice by haematoxylin-eosin staining. Molecular assays demonstrated that DS decreased mRNA and protein expression of TNF-α, IL-17A, IL-1β, and HIF-1α.

Conclusion: This study initially emphasizes the potential of DS in addressing adenomyosis by concurrently targeting an anti-inflammatory network involving the TNF-α/HIF-1α/IL-17 signaling pathways, supporting its development as a phytotherapeutic agent.

Keywords: adenomyosis, *Salvia miltiorrhiza*, drug repurposing, network pharmacology, computational analysis, multi-target, anti-inflammation pathways

Received: 28 April 2025
Accepted: 19 August 2025
Published: 22 August 2025

Introduction

Adenomyosis is a common gynecological inflammatory disorder marked by the invasion of endometrial glands and stroma into the uterine myometrium. It is strongly associated with reduced fertility potential.[1] The advent of sophisticated imaging modalities coupled with enhanced clinical expertise has led to both higher detection rates and a demonstrably younger demographic profile in adenomyosis.[2] Research indicates that adenomyosis affects approximately 20% of gynecology patients and may contribute to more than 40% of all hysterectomies performed.[3] Patients with adenomyosis suffer from severe anemia resulting from heavy menstrual bleeding, as well as challenges related to female infertility and adverse obstetric outcomes.[4] This condition significantly burdens patients and society, posing substantial challenges for gynecology and reproductive endocrinology specialists. Hysterectomy remains the gold-standard definitive treatment for symptomatic adenomyosis.[5] However, this approach carries substantial clinical limitations, including permanent fertility loss and potentially significant quality-of-life impairments. Current conservative surgical alternatives demonstrate considerable variability in therapeutic efficacy, with reported recurrence rates exceeding 40%.[6] The suboptimal outcomes frequently necessitate adjunctive pharmacotherapy to achieve acceptable clinical results.[7] Given these constraints, medical therapy functions as the primary first-line therapeutic strategy, especially for younger patients seeking fertility preservation. However, developing precise targeted therapeutic options still presents unresolved challenges.[8] Therefore, the development of effective therapeutic agents for adenomyosis is critically important.

Adenomyosis is known as an estrogen-dependent disease, as its growth is typically stimulated by estrogen and suppressed by progestogens.[9] Consequently, hormone-based endocrine therapies are often effective at managing their symptoms.[10] Some studies suggest that oral contraceptives or progesterone can induce decidualization and atrophy of ectopic endometrium, thereby controlling disease progression. Conversely, the basal endometrium in adenomyosis may be progesterone-resistant, making the efficacy of progesterone treatment debatable.[11] Gonadotropin releasing hormone analogs can suppress adenomyosis by inducing menopausal status, but their use is limited to short-term treatment due to side effects and high recurrence rates after discontinuation.[12] These factors pose significant challenges to current pharmacological management of adenomyosis. Therefore, a growing number of patients are seeking complementary therapeutic options, prompting specialists to investigate traditional Chinese medicine (TCM) protocols.

Emerging evidence positions TCM as a promising modality that not only modulates systemic homeostasis[13] but also addresses the chronic inflammatory nature of adenomyosis.[14–16] The accumulation of inflammatory mediators in adenomyotic lesions and their role in disease progression and symptom manifestation[17] provide a rationale for TCM's observed clinical benefits, including symptom relief, improved fertility outcomes, and reduced recurrence.[14] Mechanistic studies, such as those on Qiu's Neiyi Recipe, demonstrate TCM's capacity to regulate inflammatory cascades via the MAPK pathway.[15] And, rhein effectively alleviates adenomyosis in a dose-dependent manner by counteracting the IL-1β-induced increase in nuclear translocation of β-catenin through the inhibition of the NF-κB and β-catenin signaling pathways.[16] These findings collectively underscore the therapeutic potential of targeting inflammatory pathways with herbal medicine in adenomyosis. DS is one of the most significant medicinal plants of TCM in Chinese. Numerous studies have demonstrated that DS and its active compounds possess notable anti-inflammatory, therapeutic effects on menstrual dysregulation, antiplatelet properties, etc.[18,19] Although DS is widely used to treat various gynecological diseases, including gynecological cancers,[20,21] polycystic ovary syndrome,[22] and endometriosis,[19] the specific active compounds in DS responsible for treating adenomyosis and their mechanisms of action remain unexplored.

Understanding the pharmacology and mechanisms of action of DS is crucial for elucidating its therapeutic effects in adenomyosis, offering significant potential for developing novel treatment strategies. While the multi-component and multi-target therapeutic characteristics of herbal medicines have gained global recognition for managing complex diseases lacking specific therapies, this polypharmacological profile also poses challenges in systematically evaluating therapeutic outcomes and deciphering underlying mechanisms.[23] To address these challenges, contemporary research has adopted innovative methodologies such as serum pharmacochemistry, which has proven effective in identifying bioactive herbal components and validating their therapeutic benefits in TCM.[24] Additionally, network pharmacology has emerged as a powerful tool for analyzing complex interactions among drugs, diseases, and targets, enabling a holistic assessment of multi-component and multi-pathway effects.[25] This approach is instrumental in modern TCM research, advancing investigations into the safety,

efficacy, and mechanistic basis of herbal therapies, thereby enhancing their scientific credibility and clinical acceptance.[26] Despite these advancements, network pharmacology applications in adenomyosis research remain limited, with no studies to date exploring the mechanisms of DS in treating adenomyosis using this approach.

This study aims to elucidate the multi-target mechanisms by which DS ameliorates adenomyosis through an integrative pharmacological approach that combines computational prediction methods (network pharmacology, molecular docking, and molecular dynamics simulations) with multimodal experimental validation techniques (serum pharmacochemistry, transcriptomics, and in vivo assays). The results indicate that DS exerts significant anti-inflammatory effects by synergistically inhibiting the TNF-α/IL-17/HIF-1α signaling pathways and TNF-α/IL-1β activation. These findings provide new insights into the use of TCM for treating adenomyosis and offer theoretical guidance for future experimental research and clinical applications. Figure 1 illustrates the study workflow evaluating the therapeutic effects of DS on adenomyosis.

Materials and Methods

Drugs and Chemical Reagents

DS was purchased from Kangmei Pharmaceutical Co., Ltd (Guangdong, China). Ultra-high liquid chromatography (Thermo Fisher Scientific, Model: Vanquish Flex UHPLC). High-resolution mass spectrometer (Q Exactive HFX, Thermo, USA). Chromatographic column (Waters HSS T3 (100×2.1 mm, 1.8 μm)). High-speed freeze centrifuge (Hettich, Germany, model: Mikro 220R), Ultrasonic extractor (Kunshan Ultrasonic Instrument Co., Ltd., model: KQ3200D). Antibodies mentioned in the experiments included tumor necrosis factor-α (TNF-α, Affinity, AF7014), interleukin-17A (IL-17A, Affinity, DF6127), interleukin-1β (IL-1β, Affinity, AF5103), hypoxia-inducible factor-1α, (HIF-1α, Affinity, AF1009), glyceraldehyde-3-phosphate dehydrogenase (GAPDH Affinity, AF7021), β-actin (Affinity, AF7018).

Sample Preparation of DS Extract

The extraction of DS was performed according to a previously established method.[27] Briefly, 90% ethanol was added to DS and refluxed for 1.5 hours, followed by filtration and recovering the ethanol from the filtrate to a thick paste. Boil the medicinal residue in water for 1 hour, filter, and combine the filtration with the aforementioned thick paste. Concentrate under reduced pressure to 1g/mL. Take 200 μL of DS extract sample, add 600 μL of methanol, sonicate for 30 minutes, and centrifuge at 4°C and 12000 rpm for 10 minutes. Take 100 μL of solution and place it in an injection bottle for testing.

Establishment of the Adenomyosis Model and Serum Sample Processing

Thirty ICR mice were maintained in an SPF environment of 22 ± 2°C and 40–70% humidity. All experimental procedures involving animals were reviewed and approved by the Experimental Animal Ethics Committee of Fujian Medical University (Approval NO. IACUC-FJMU-2023-Y-0804) in strict accordance with the national standard "Guidelines for Ethical Review of Animal Welfare" (GB/T 35892–2018) of China. After one week of acclimatization, all mice were randomly divided into six groups (n = 6): control (Saline solution daily), model, positive drug (Gestrinone, 0.325mg/kg, Twice a week), and drug intervention groups (7.8 g/kg for the high-dose group [DS-H], 3.9 g/kg for the medium-dose group [DS-M], and 1.3 g/kg for the low-dose group [DS-L]). The doses of DS were determined through literature review and clinical evidence,[28] showing: 1) Clinical danshen dosage ranges 10–37.3 g/day; 2) Function-dependent variations exist: blood circulation (12–30 g), pain relief (10–37.3 g), abscess treatment (15–30 g), and sedation (10–15 g). Considering adenomyosis' "blood stasis and internal obstruction" pathology, we selected three human-equivalent doses (15, 30, 60 g) converted to mouse doses (1.3, 3.9, 7.8 g/kg) using body surface area normalization (70 kg human × 9.1 conversion factor). These doses, proven effective in other disease models,[29] were well below safety thresholds (80 mg/kg) and toxicity levels (320 mg/kg), ensuring intervention safety.[30] Select age-matched ICR male mice, euthanize them, and perform a craniotomy to extract the pituitary gland, creating a pituitary saline suspension; for female mice, administer propofol injection at a dose of 0.1 mg/g via intraperitoneal injection for anesthesia, sterilize the lower abdomen, make a 2 cm longitudinal incision slightly to the right of the midline, isolate the right uterus, and use a catheter to inject the pituitary saline suspension intrauterine, followed by the

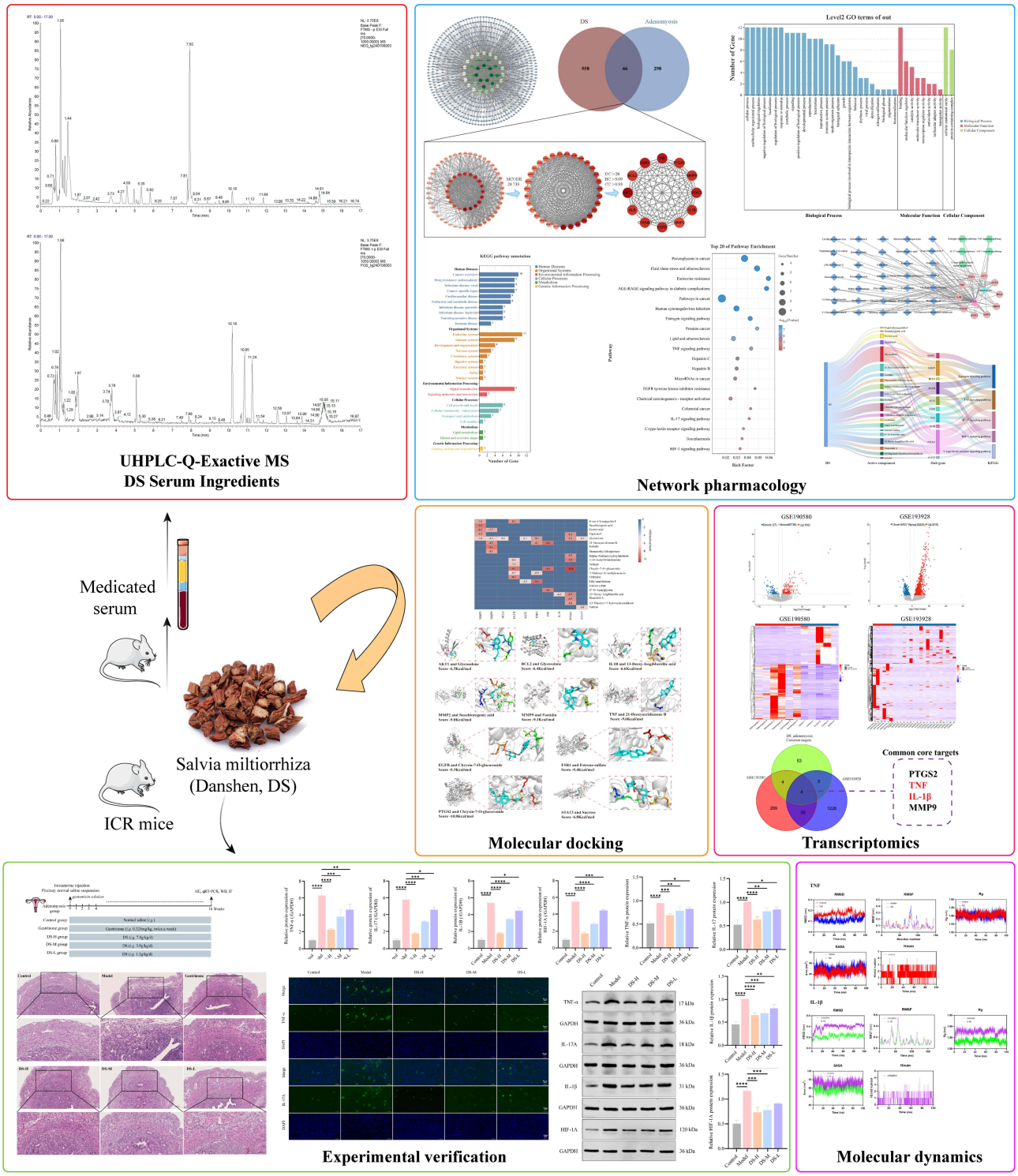

Figure 1 Workflow for studying the mechanisms of DS in treating adenomyosis.

application of gentamicin solution (0.25 mL, 10000 U) to prevent infection. In the identification IAIBs of DS group, the gastric dose of DS was 100 mg/kg/d, the blank group was gavage for 7 days, fasting for 12 hours before the last time, anesthesia for 1 hour, cardiac blood was collected, packaged in a centrifuge tube without sodium heparin, stand for 1 hour, 4°C, 3000 rpm centrifugation for 10minutes, the upper serum was divided and stored in −80 °C.

UPLC and MS Conditions

Chromatography conditions: Column: Waters HSS T3 (1002.1 mm, 1.8 μm); Mobile phase A (0.1% formic acid in water) and B (0.1% formic acid in acetonitrile); Flow rate 0.3 mL/min, column temp 40°C, injection volume 2 μL. Elution gradient: 0 min A phase/B phase (100:0, v/v), 1 min Phase A/B phase (100:0, v/v), 12 min A/B (5:95, v/v), 13 min Phase A/Phase B. (5:95, v/v), 13.1 min Phase A/Phase B (100:0, v/v), 17 min Phase A/B Phase (100:0, v/v). Mass spectrometry conditions: the primary and secondary maps were collected using the Thermo Q Exactive HFX high-resolution mass spectrometry system, equipped with electric spray ion source (ESI), sheath gas 40 arb, auxiliary gas 10 arb, ion spray voltage+3000 V/-2800 V, temperature 350°C, ion transport tube temperature 320°C. The scanning mode was Full-ms-ddMS 2 and scanned in positive/negative ions. The scanning range of primary mass spectrometry is 70–1050 Da, with a primary resolution of 70000 and a secondary resolution of 17500, collision energy 10/30/60 V.

Disease Target Screening

Thirty-five compounds were identified, and 2D structures were sourced from PubChem (https://pubchem.ncbi.nlm.nih.gov/). Targets were gathered via Swiss target prediction (http://www.swisstargetprediction.ch/). GeneCards (https://www.genecards.org/), OMIM (https://www.omim.org/) and PharmgKB (https://www.pharmgkb.org/) searched for "Adenomyosis" targets. Venn tool identified intersections of compound targets.

Protein–Protein Interaction (PPI) Analysis and Screening of Core Interacting Genes

The shared target genes between DS components and adenomyosis were analyzed using the STRING 10.5 database (https://cn.string-db.org/) for conducting PPI network analysis, with the species parameter set to "Homo sapiens." The interaction threshold was configured to "medium confidence (> 0.4)", while other parameters were maintained at their default settings. The resulting interaction data were exported in TSV format and imported into Cytoscape 3.7.2 for network construction. During this process, isolated nodes were systematically removed to refine the network. Module analysis using the MCODE plugin identified densely connected regions, with the highest-scoring module chosen for further investigation.[31] For the identification of key molecular hubs, the CytoNCA plugin was employed to extract the top core interacting targets based on network centrality measures.

Enrichment Analysis and Network Pharmacology Analysis

Analysis of these core interacting targets through Gene Ontology (GO) and Kyoto Encyclopedia of Genes and Genomes (KEGG) enrichment analysis was conducted in DENOVO (https://www.omicshare.com),[32] setting $p < 0.05$ as the threshold to exclude cellular components (CC), biological processes (BP), molecular functions (MF), and enrichment pathways.

Network Pharmacology Analysis and Construct Core Pathway-Target Network for DS Treatment of Adenomyosis

To elucidate the intricate relationships among "herbs-compounds-targets-pathways", we incorporated the common core target genes from DS active components and adenomyosis into Cytoscape 3.7.2 for detailed analysis. Through KEGG enrichment analysis, we initially identified key pathways involved in the efficacy of DS against adenomyosis and subsequently mapped the core targets associated with these pathways. We then pinpointed the DS active compounds that correspond to the identified core targets. Leveraging the analytical capabilities of Cytoscape 3.7.2, we established the "DS Components-Targets-Adenomyosis-Pathways" network, aiming to comprehensively elucidate the underlying mechanisms of DS's therapeutic action in adenomyosis.

Molecular Docking Analysis

The crystal structure of the core proteins was obtained from the Protein Database (PDB) database (http://www.rcsb.org/). The core compounds in the network diagram of "DS-Active Compounds-Intersection Targets" were obtained in SDF file format from the PubChem database (https://pubchem.ncbi.nlm.nih.gov/) to download. OpenBabel software was used to convert the SDF file into mol2 format. AutoDock Tool software[33] performed hydrogenation, ligand detection, and other operations before

saving it in pdbqt format. Pymol software[34] removed its ligands and water molecules. The binding energy was calculated in Autodock-1.5.7 software. PyMol-2.5.2 software visualized the docking results. Binding energy values indicate the affinity of the active compound for its protein targets. The stability of ligand-receptor binding was inversely correlated with binding energy.[35]

Adenomyosis Datasets Acquisition and Target Validation by Transcriptomic Analysis

Transcriptomic analysis of two adenomyosis datasets, GSE193928 and GSE190580, was conducted using differential expression analysis from the Gene Expression Omnibus database (GEO: https://www.ncbi.nlm.nih.gov/geo/), following established research methods.[36] The "limma" R package was used, setting threshold values at $|logFC| > 2.0$ and $P < 0.05$ to identify significant differential expression. The results were visualized using volcano plots and heatmaps, created with the "ggplot2" and "pheatmap" R packages, respectively. Additionally, a Venn diagram was employed to identify common targets between the potential targets of DS-adenomyosis and those found in the two adenomyosis datasets.

Molecular Dynamics Simulation

This study performed all-atom Molecular dynamics (MD) simulations on the protein-ligand complexes derived from molecular docking using GROMACS 2022.4. The AMBER14SB force field was applied to parameterize the protein, while the topology files for small molecules were generated using ACPYPE and Antechamber tools. The system was solvated in a cubic water box with a 1 nm buffer distance between the complex and box edges, utilizing the TIP3P water model. Sodium and chloride ions were added to neutralize the system charge. The energy minimization was conducted via the steepest descent algorithm, followed by temperature equilibration (300 K) under the NVT ensemble and pressure equilibration (101.325 kPa) under the NPT ensemble. Subsequently, production MD simulations were carried out for 100 ns at 300 K, generating 10,000 trajectory frames. Key structural and interaction parameters, including root-mean-square deviation (RMSD), root-mean-square fluctuation (RMSF), solvent-accessible surface area (SASA), radius of gyration (Rg), and intermolecular hydrogen bond dynamics, were systematically analyzed from the trajectories. Higher RMSD values and large-amplitude fluctuations indicate increased conformational flexibility, while lower RMSD values suggest improved structural stability throughout the simulation trajectory. The RMSF is a key metric for assessing local flexibility in molecular dynamics simulations.[37]

Hematoxylin and Eosin Stain

Mice uterine tissues were collected and fixed in 4% paraformaldehyde, dehydrated through a graded series of ethanol, cleared with xylene, and embedded using an embedding machine. Sections of 5μm thickness were cut and stained with hematoxylin and eosin (H&E). The histological changes were observed under a light microscope at 200× and 400× magnifications.

Quantitative Real-Time Polymerase Chain Reaction (qRT-PCR)

Cellular RNA was extracted with Trizol (Invitrogen, USA) per the manufacturer protocol. cDNA was synthesized using the PrimeScript RT kit (Biosharp, China). mRNA levels of GAPDH, TNF-α, IL-17A, IL-1β, and HIF-1α were quantified by qPCR with SYBR Premix Ex Taq (Biosharp, China). Primer sequences are in Table 1, verified by BLAST for specificity. Data were normalized to GAPDH and analyzed using the $2^{(-\Delta\Delta CT)}$ method.

Western Blot (WB) Analysis

Proteins from uterine tissue were extracted using RIPA buffer (Beyotime, China). They were separated via SDS-PAGE, transferred to PVDF membranes, and blocked with 5% milk at room temp. Incubate the cell membrane overnight with primary antibodies including TNF-α (1:500), IL-17A (1:500), IL-1β (1:1000), and HIF-1α (1:1000) at 4°C. Subsequently, the membrane was incubated with HRP conjugated secondary antibody at room temperature for 1 hour. ECL Plus (Thermoscience) was used for detection, and Image J for densitometry analysis.

Table 1 Primer Sequence

Gene	Primer
TNF-α	Forward 5′-CAGGCGGTGCCTATGTCTC-3′
	Reverse 5′-CGATCACCCCGAAGTTCAGTAG-3′
IL-17	Forward 5′-TCAGCGTGTCCAAACACTGAG-3′
	Reverse 5′-CGCCAAGGGAGTTAAAGACTT-3′
IL-1β	Forward 5′-GAAATGCCACCTTTTGACAGTG-3′
	Reverse 5′-TGGATGCTCTCATCAGGACAG-3′
HIF-1A	Forward 5′-TCTCGGCGAAGCAAAGAGTC-3′
	Reverse 5′-AGCCATCTAGGGCTTTCAGATAA-3′
GAPDH	Forward 5′-AGGTCGGTGTGAACGGATTTG-3′
	Reverse 5′-GGGGTCGTTGATGGCAACA-3′

Immunofluorescence (IF) Analysis

For IF analysis, paraffin-embedded sections of Uterine tissue were incubated with primary detection antibody TNF-α (1:200) and IL-17A (1:30) at 4°C, followed by a fluorescent secondary antibody for 1 h in the dark. Sections were counter-stained with DAPI and viewed under a fluorescent microscope (Leica DMi8, Solms, Germany).

Statistical Analysis

SPSS 26.0 statistical software was used to analyze the data. All data plots were processed using Graphpad Prism 9.0.0 (Graphpad Software, La Jolla, CA) software. For comparisons involving more than two groups, ANOVA followed by LSD test was applied. All data were represented as mean ± standard deviation (SD) and $p < 0.05$ was considered statistically different. Statistical analysis was performed by one-way analysis of variance (ANOVA) tests. Each experiment was repeated at least three times independently to confirm the consistency of the findings. The level of statistical significance was set at $p < 0.05$ for all analyses. Significance levels in the figures were denoted as follows: $p < 0.05$ (*), $p < 0.01$ (**), $p < 0.001$ (***), and $p < 0.0001$ (****).

Results

Identification of DS Components in Blood

UHPLC-MS analysis successfully identified and characterized 35 potential IAIBs in DS, including 8-epi-Chlorajapolide F, 21-Deoxyneridienone B, Neochlorogenic acid, 8alpha-Methacryloyloxybalchanin, and 1-O-Acetyl britannilactone et al. The comprehensive analytical data, including compound name, retention time (RT), ionization mode, adduct formation patterns, molecular formula, observed m/z values, and fragmentation scores, were systematically documented and statistically analyzed in Figure 2 and Table 2. This high-resolution mass spectrometry-based characterization provides the detailed chemical profile of DS-derived bioactive components, establishing a robust foundation for subsequent pharmacological investigations.

Identification of Intersection Targets and Screening of the Core Targets

To construct the compound-putative target network of DS, we first analyzed 35 compounds and 624 hypothesized targets in DS, and the interactions were identified and visualized as the herb-compound-target network, which contained 660 nodes and 1618 edges in Cytoscape 3.7.2 (Figure 3A). Potential adenomyosis targets were identified from GeneCards (364 targets), OMIM (1 target), and PharmGKB (4 targets). After duplication, 367 unique targets were retained for further analysis. Using a Venn diagram tool, we intersected the DS and adenomyosis targets and identified 66 common targets (Figure 3B and Supplementary Table 1).

The PPI network comprised 66 nodes and 106 edges, with an average node degree of 3.21. The network demonstrated significant PPI enrichment (p-value < 1.0e-16), indicating that the interacting genes had substantially more connections among themselves than would be expected for a randomly selected gene set of the same size and degree distribution from

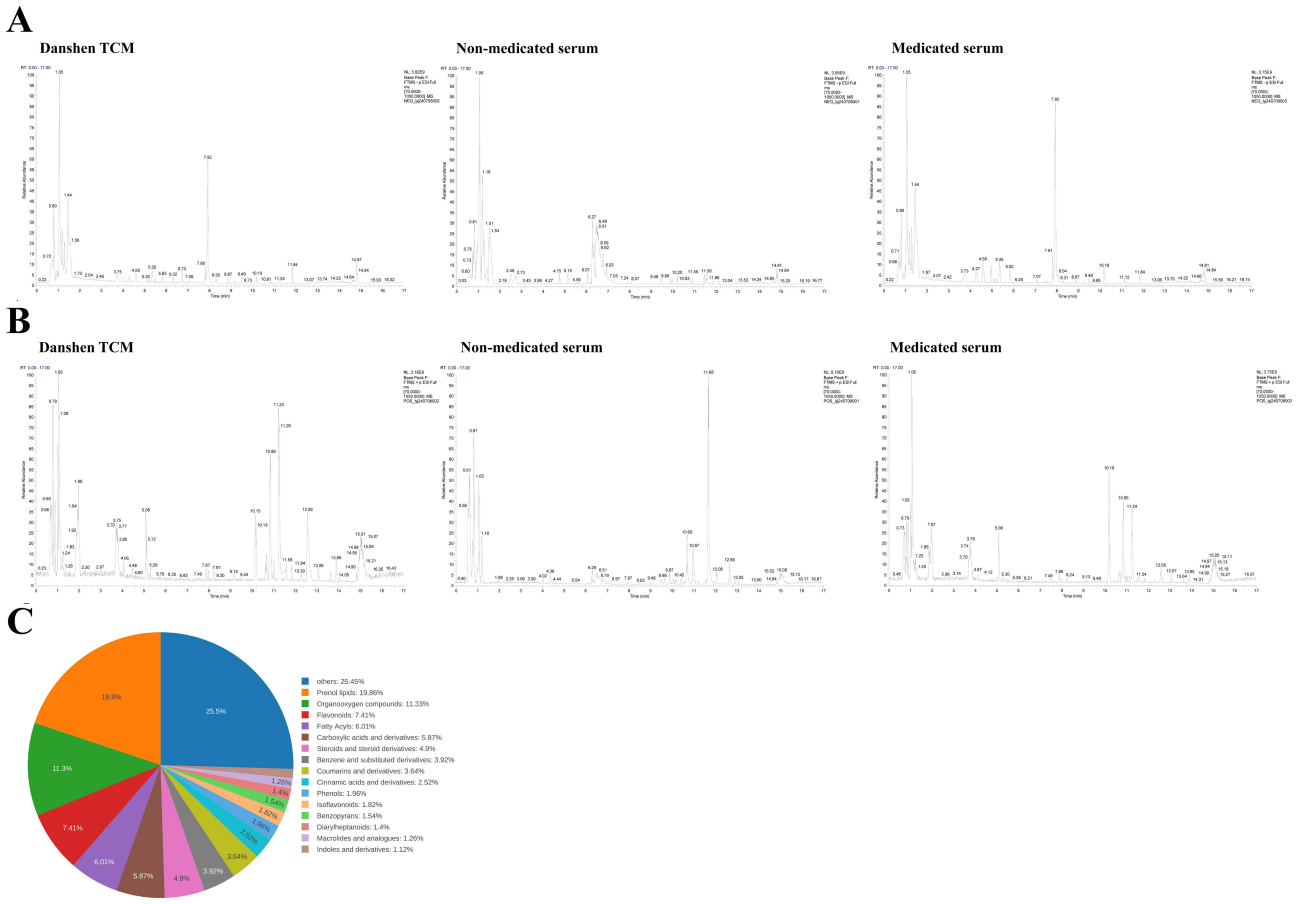

Figure 2 Ingredients of DS containing serum detected by UHPLC-MS. (**A**) DS TCM, Non-medicated serum, and medicated serum samples (negative ion mode). (**B**) DS TCM, Non-medicated serum, and medicated serum samples (positive ion mode). (**C**) Pie chart of serum metabolite classification.

the genome. This significant enrichment suggests that these genes are biologically interconnected and potential function as a cohesive group in the context of drug screening DS for the treatment of adenomyosis. Such analysis offers critical mechanistic insights into the therapeutic potential of DS for adenomyosis treatment.[38]

After eliminating isolated and disconnected genes, the remaining interconnected targets were imported into Cytoscape 3.7.2 for visualization and further topological analysis. This process generated a comprehensive PPI network diagram, facilitating the exploration of interaction networks (Figure 3C). The module analysis of the MCODE plugin identified the clustering module with the highest score, with an MCODE score of 24.733. The clustering hub module of the 31 targets is the core target for DS therapy of Adenomosis (Figure 3D). Subsequently, through rigorous network topology analysis employing predefined screening criteria (degree centrality (DC) > 28, betweenness centrality (BC) > 9.09, closeness centrality (CC) > 0.93), we systematically identified 12 core therapeutic targets (Figure 3E). These pivotal targets include *TNF, IL1β, MMP2, ESR1, PTGS2, STAT3, BCL2, AKT1, MMP9, ALB, CTNNB1*, and *EGFR*, collectively representing 18.18% of the total number of targets. The complete topological parameters for these key targets are presented in Table 3.

Gene Ontology and KEGG Pathway Analysis

Functional enrichment analysis of the 12 core therapeutic targets in DS-adenomyosis interaction network systematically performed GO and KEGG pathway analyses. The GO enrichment analysis mainly functions through biological processes (BP), molecular functions (MF), and cellular components (CC). The analysis identified a total of 3,139 GO terms, with 2,458 (78.3%) reaching statistical significance. GO-BP contained most terms (2,736 total, 2,240 significant), representing 91.13% of all significant GO terms; GO-MF comprised 200 terms (118 significant, 4.8% of significant GO terms); GO-CC included 203 terms (100 significant, 4.07% of significant GO terms). DS-adenomyosis core therapeutic targets

Table 2 Thirty-Five IAIBs Identified from DS

No.	Compound Name	m/z	RT (min)	Mode	Adducts	Formula	Fragmentation Score
1	8-epi-Chlorajapolide F	297.1135393	10.21878333	neg	M+Na-2H	$C_{16}H_{20}O_4$	88.6
2	21-Deoxyneridienone B	373.2026137	10.96355	neg	M+FA-H	$C_{21}H_{28}O_3$	86.5
3	Neochlorogenic acid	353.0883516	5.822633333	neg	M-H	$C_{16}H_{18}O_9$	84
4	8alpha-Methacryloyloxybalchanin	313.1445245	10.92606667	neg	M-H2O-H	$C_{19}H_{24}O_5$	83
5	1-O-Acetyl britannilactone	289.1444651	11.21623333	neg	M-H2O-H	$C_{17}H_{24}O_5$	81.7
6	Foetidin	331.1918445	10.25463333	neg	M-H, M+Cl	$C_{20}H_{28}O_4$	81.6
7	13-Deoxy-Isogibberellic acid	329.1398533	9.884816667	neg	M-H	$C_{19}H_{22}O_5$	81.1
8	Lysofungin	595.2898083	14.82545	neg	M-H	$C_{27}H_{49}O_{12}P$	80.9
9	Effusanin B	371.1870339	10.5752	neg	M-H2O-H	$C_{22}H_{30}O_6$	79.9
10	Estrone sulfate	253.1582688	10.20326667	pos	M+H-H2O	$C_{18}H_{22}O_2$	78.1
11	Tagitinin F	313.1428926	8.0611	pos	M+H-2H2O	$C_{19}H_{24}O_6$	77.5
12	Chlorantholide E	299.0927631	8.079933333	neg	M+Na-2H	$C_{15}H_{18}O_5$	77
13	Daucoidin A	325.1085895	9.884816667	neg	M-H2O-H	$C_{19}H_{20}O_6$	75.5
14	sucrose	341.1094917	1.136366667	neg	M-H, M+Cl	$C_{12}H_{22}O_{11}$	73.7
15	Ethyl arachidonate	350.3048373	10.8563	pos	M+NH4	$C_{22}H_{36}O_2$	72.9
16	3,5-Diprenyl-4-hydroxybenzaldehyde	239.1442279	9.479516667	neg	M-H2O-H	$C_{17}H_{22}O_2$	72.8
17	Gluconic acid	231.0278593	0.785466667	neg	M+Cl	$C_6H_{12}O_7$	71.7
18	Norpterosin B	203.1080567	8.410266667	neg	M-H	$C_{13}H_{16}O_2$	71
19	(2R,3S)-Pterosin C	199.1114842	10.80656667	pos	M+H-2H2O	$C_{14}H_{18}O_3$	70
20	Monomethyl lithospermate	551.117,9927	6.79815	neg	M-H	$C_{28}H_{24}O_{12}$	68.8
21	Toddanol	311.092629	8.835316667	neg	M+Na-2H	$C_{16}H_{18}O_5$	68.1
22	Evernic acid	377.0883516	5.128	neg	M-H, M+FA-H	$C_{17}H_{16}O_7$	66.6
23	6′-O-Acetylglycitin	509.1089692	6.132816667	neg	M+Na-2H	$C_{24}H_{24}O_{11}$	65.1
24	8-Hydroxythymol	331.1917385	11.10555	neg	2M-H	$C_{10}H_{14}O_2$	64.4
25	Toddalolactone 3-O-methyl ether	343.1193302	7.7395	neg	M+Na-2H	$C_{17}H_{22}O_6$	64.1
26	Stearic acid amide	325.3206714	11.08583333	pos	M+ACN+H	$C_{18}H_{37}NO$	63.1
27	7,8-Dihydrokawain-5-ol	247.0976718	8.410266667	neg	M-H	$C_{14}H_{16}O_4$	61.4
28	Kainic acid	236.0914016	0.892116667	pos	M+Na	$C_{10}H_{15}NO_4$	59.6
29	Syringin	417.1406351	4.68075	neg	M+FA-H	$C_{17}H_{24}O_9$	58.8
30	Chrysin-7-O-glucuronide	475.0885247	5.891816667	neg	M+FA-H	$C_{21}H_{18}O_{10}$	57.6
31	Methyl isodrimeninol	271.1701485	10.8218	neg	M+Na-2H	$C_{16}H_{26}O_2$	55.2
32	7-Methoxy-4-methylcoumarin	235.0613522	5.250266667	neg	M-H, M+FA-H	$C_{11}H_{10}O_3$	54.6
33	Glycosolone	296.1275976	9.841	pos	M+Na	$C_{16}H_{19}NO_3$	53.4
34	Crebanine	372.1798724	9.886883333	pos	M+CH3OH+H	$C_{20}H_{21}NO_4$	52.1
35	Stepharine	296.1296352	10.06435	neg	M-H	$C_{18}H_{19}NO_3$	50.2

involved in BP mainly include cellular progress, immune system process, biological regulation, biological adhesion, growth, and response to stimulus (Figure 4A). These findings collectively suggest that DS may exert its therapeutic effects on adenomyosis by acting on key targets involved in multi-level regulation of these fundamental BP.

KEGG enrichment analysis identified a total of 174 signaling pathways corresponding to12 core targets, of which 109 (62.64%) were statistically significant. The most enriched pathways in Human Diseases were associated with cancer, diabetic complications, and infectious diseases, reflecting the inflammatory and proliferative nature of AM. Pathways in Organismal Systems involved in endocrine and immune regulation were prominent, including: Estrogen signaling pathway (Q=4.34e-07), IL-17 signaling pathway (Q=7.67e-05), and C-type lectin receptor signaling pathway (Q=1.24E-04); Key pathways in Environmental Information Processing regulating inflammatory and stress responses: TNF-α signaling pathway (Q=5.72e-06), HIF-1α signaling pathway (Q=1.58e-04) (Figure 4B). The top 20 signal pathways are shown in the bubble diagram (Figure 4C). These results strongly suggest that DS exerts therapeutic effects

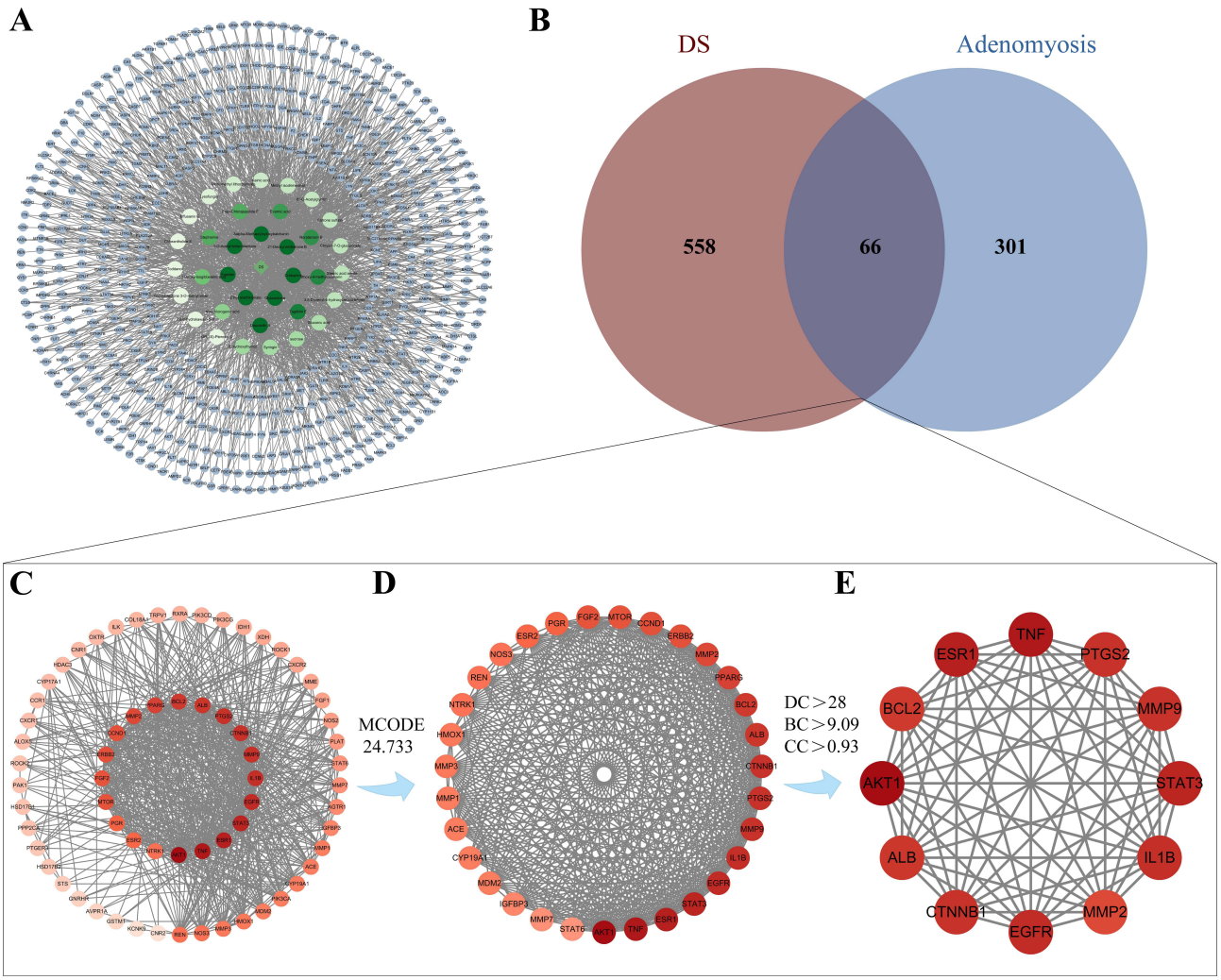

Figure 3 DS and adenomyosis cross-core target analysis. (**A**) DS-Compound-Target network diagram. (**B**) Venn diagram of DS and adenomyosis for identification of intersection targets. (**C**) PPI network diagram of intersecting targets. (**D**) MCODE analysis DS-adenomyosis of PPI network for screening of the core targets. (**E**) Top 12 core targets.

on adenomyosis through multi-pathway modulation, primarily targeting inflammation, hormone signaling, and tissue remodeling processes. Given that adenomyosis is characterized as an estrogen-dependent chronic inflammatory process with abundant inflammatory mediators in adenomyotic lesions,[39–41] our pathway analysis revealed five particularly

Table 3 Information on 12 Core Interaction Targets and Its Topological Parameters

NO.	Gene	Full Name	Degree	Betweenness	Closeness
1	*STAT3*	Signal transducer and activator of transcription 3	30	13.069386	1
2	*BCL2*	Apoptosis regulator Bcl-2	30	13.069386	1
3	*AKT1*	AKT Serine/Threonine Kinase 1	30	13.069386	1
4	*TNF*	Tumor necrosis factor superfamily	30	13.069386	1
5	*MMP2*	Matrix metalloproteinase-2	29	10.9052	0.9677419
6	*IL1β*	Interleukin-1 beta	29	11.507224	0.9677419
7	*ESR1*	Estrogen receptor alpha	29	10.959687	0.9677419
8	*PTGS2*	Prostaglandin G/H synthase 2	29	11.5540495	0.9677419
9	*MMP9*	Matrix metalloproteinase-9	29	10.9052	0.9677419
10	*ALB*	Albumin	29	10.959687	0.9677419
11	*CTNNB1*	Catenin beta 1	29	11.534021	0.9677419
12	*EGFR*	Epidermal growth factor receptor	28	9.093922	0.9375

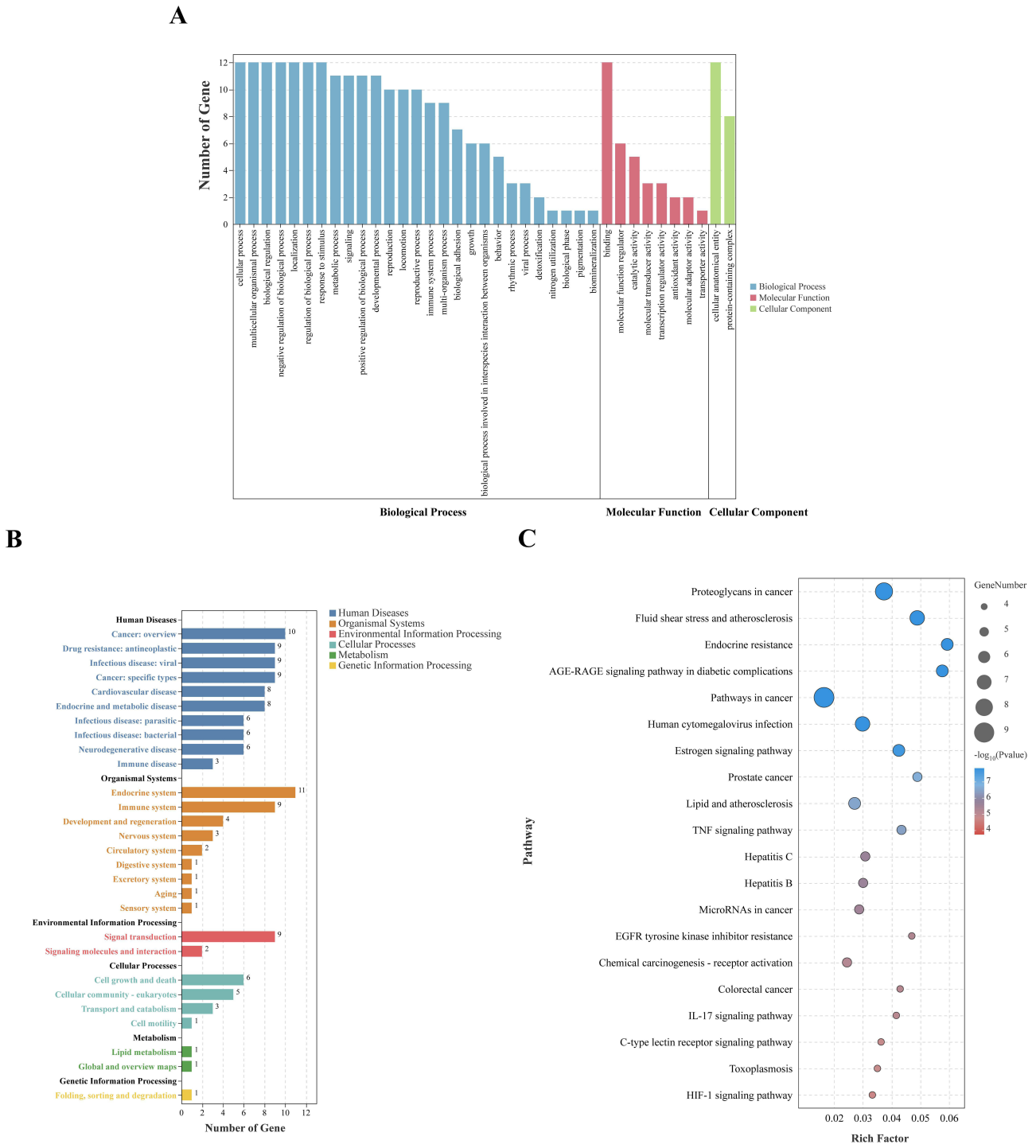

Figure 4 Core target bioinformatics analysis. (**A**) Gene ontology functional analysis. (**B**) KEGG Pathway annotation, and (**C**) Top 20 KEGG Pathway Enrichment.

significant inflammatory-related signaling pathways that are predicted to be key mediators of DS's therapeutic effects: Estrogen signaling pathway, TNF-α signaling pathway, IL-17 signaling pathway, C-type receptor signaling pathway, and HIF1-α signaling pathway. This comprehensive analysis not only highlights the most relevant pathways involved in DS's action against adenomyosis but also reveals the multi-target mechanisms underlying its therapeutic potential for adenomyosis.[42]

https://doi.org/10.2147/JIR.S537221

Major Pathway-Target Network for DS Treatment of Adenomyosis

Based on the five identified key DS-adenomyosis pathways, we constructed an integrated "DS- Components- Targets - Adenomyosis -Pathways" network (Figure 5A). This analysis provides a systematic demonstration of the therapeutic efficacy of DS, achieved through the synchronized regulation of functional targets, regulatory genes, and signaling pathways. Identification of five key pathways corresponding to core targets: *TNF, IL1β, MMP2, ESR1, PTGS2, STAT3, BCL2, AKT1, MMP9*, and *EGFR*. Furthermore, a sankey diagram was employed to visualize the quantitative relationships among hub genes, core pathways, and active compounds (Figure 5B). Notably, both IL-1β and TNF were identified as critical regulatory nodes concurrently involved in the TNF-α, IL-17, and HIF-1α signaling pathways. This finding provides novel insights into the multi-target mechanisms through which DS may treat adenomyosis, particularly highlighting its potential to simultaneously modulate multiple inflammatory pathways and providing a theoretical foundation for subsequent experimental validation and drug development.

Verification and Visualization of the Molecular Docking

Molecular docking analysis was used further to validate to characterize the binding interactions between the bioactive components of DS and key core targets. Based on sankey diagram screening, our analysis revealed robust binding interactions of the 10 core target proteins and corresponding bioactive components of DS (Figure 6A), with all binding energies < −5.0 kcal/mol and an average binding affinity approaching −8.0 kcal/mol, and the corresponding bioactive compounds were presented in Table 4. The compound Chrysin-7-O-glucuronide exhibited the highest binding affinity with PTGS2 (−10.8 kcal/mol). Closely following were 21-Deoxyneridienone B with TNF (−9.6 kcal/mol), Estrone sulfate with ESR1 (−9.4 kcal/mol), and Chrysin-7-O-glucuronide with EGFR (−9.3 kcal/mol). For visualization, the conformation with the lowest binding energy was selected for multi-ligand targets. In the case of single-ligand targets, which included only two, namely BCL2 with Glycosolone and IL1β with 13-Deoxy-Isogibberellic acid, the complex structures were used, having binding energies of −6.4 kcal/mol and −6.6 kcal/mol, respectively (Figure 6B). These findings suggest that the bioactive compounds of DS effectively bind to the active sites of these hub targets, highlighting their potential in treating adenomyosis through these targets.

Validation of Targets Related to DS with Adenomyosis Datasets from GEO

Transcriptomic profiling was carried out on adenomyosis-related datasets of GEO database (GSE193928 and GSE190580), Using the "limma" R package to identify potential targets (Supplementary Tables 2 and 3). The differentially expressed genes (DEGs) were visualized with volcano plots, where red dots indicated up-regulated genes and blue dots represented down-regulated ones (Figure 7A). A heatmap showcased the distribution of DEGs, emphasizing across different groups (Figure 7B). Integration of drug-target and disease-gene analyses identified *PTGS2, IL-1β, TNF*, and *MMP9* as core genes (Figure 7C). Combined with the network pharmacology findings, *IL-1β* and *TNF* were confirmed as hub nodes regulating the TNF, IL-17, and HIF-1α signaling pathways. Overall, these results confirm that DS exert therapeutic effects on adenomyosis through targeting *TNF* and *IL-1β*. This integrative multi-omics approach offers valuable insights into the molecular mechanisms underlying DS's multi-target therapeutic efficacy.

Selection of Core Targets and Bioactive Compounds for Molecular Dynamics Simulations

Since molecular docking only provides a static interaction state between compounds and proteins,[43] we further conducted 100 ns MD simulations to explore the dynamic movement and stability of key targets with the DS active components (TNF-21-deoxyneridienone B, and IL-1β-13-Deoxy-Isogibberellic acid), ensuring the feasibility of investigation into DS-adenomyosis therapeutic potential. The TNF complex (Figure 8A) exhibited stable RMSD (1.5–2.0 Å), showing a mild increase compared to unliganded TNF (1.0–1.5 Å) while maintaining an overall low fluctuation threshold (<2.0 Å), indicative of limited conformational adjustments upon ligand binding. The complex exhibited RMSF fluctuations similar to unbound TNF, with the majority of residues displaying modest fluctuations (0.5–2.0 Å), indicating well-maintained global backbone stability. RMSF profiling revealed a characteristic flexibility peak (4.0–4.3 Å) at residues 75–85, likely

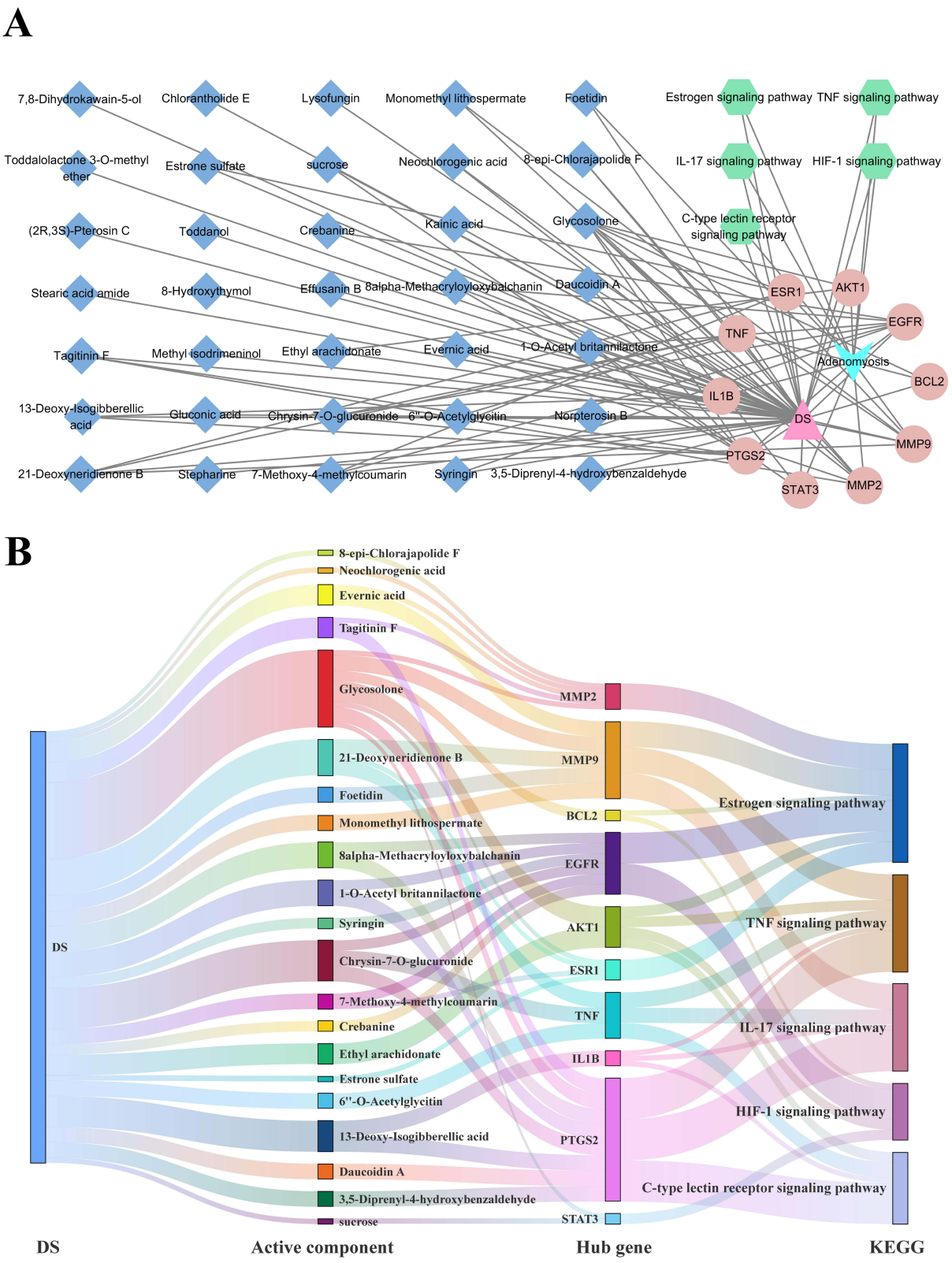

Figure 5 Major pathway-target network of DS in the treatment of adenomyosis. (**A**) "DS-Components-Targets-Signaling pathways-Adenomyosis" network diagram based on major pathway-target. (**B**) Sankey diagram of major pathway-core targets- key components of DS for adenomyosis.

https://doi.org/10.2147/JIR.S537221

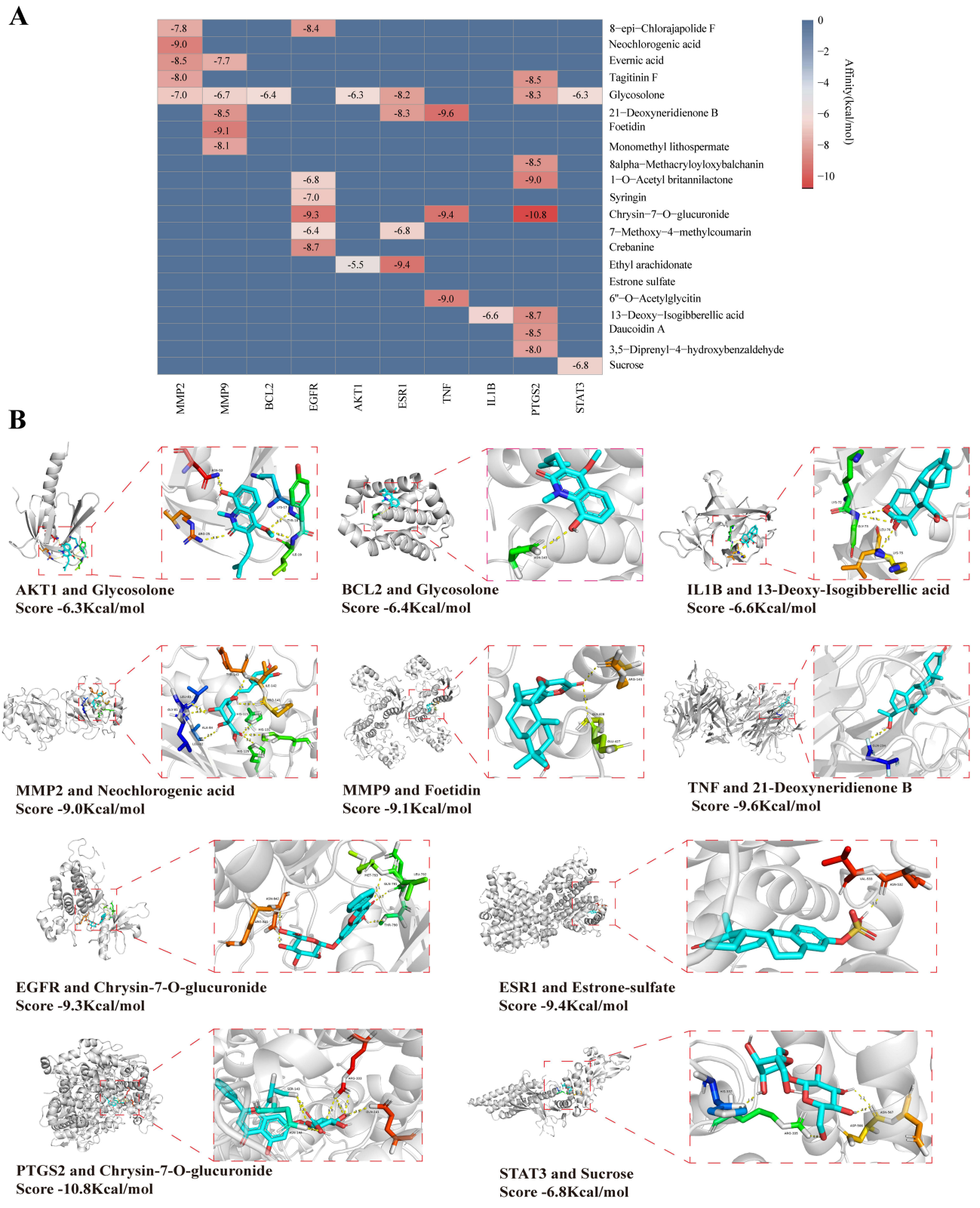

Figure 6 Validation and screening of molecular docking. (**A**) Molecular docking hotspot map of core targets and key components. Binding energies (kcal/mol) of core targets and active compounds of DS. (**B**) Docking patterns of core targets and active compounds of adenomyosis.

Table 4 Details of the Compounds in the Compound-Core Target-Key Pathway Network of DS-Adenomyosis

NO.	Component Name	PubChem CID	Molecular Weight g/mol	CAS	CHEBI/ChEMBL ID
1	8-epi-Chlorajapolide F	131676071	276.33	863301-69-3	CHEBI:3960896
2	Neochlorogenic acid	5280633	354.31	906-33-2	CHEBI:16384
3	Evernic acid	10829	332.3	537-09-7	CHEBI:111284
4	Tagitinin F	5281501	348.4	59979-57-6	CHEBI:9390
5	Glycosolone	155059	273.33	67879-81-6	–
6	21-Deoxyneridienone B	16104854	328.4	924910-83-8	CHEMBL376854
7	Foetidin	15945065	382.5	89900-57-2	CHEMBL1362201
8	Monomethyl lithospermate	25256837	552.5	933054-33-2	CHEMBL473868
9	8alpha-Methacryloyloxybalchanin	102004556	332.4	104021-39-8	–
10	1-O-Acetyl britannilactone	25018668	308.4	681457-46-5	CHEMBL274543
11	Syringin	5316860	372.37	118-34-3	CHEBI:9380
12	Chrysin-7-O-glucuronide	14135335	430.4	35775-49-6	CHEBI:181485
13	7-Methoxy-4-methylcoumarin	390807	190.19	2555-28-4	CHEBI:107662
14	Crebanine	159999	339.4	25127-29-1	CHEBI:228860
15	Ethyl arachidonate	5367369	332.52	1808-26-0	CHEBI:84873
16	Estrone sulfate	3001028	350.4	481-97-0	CHEBI:17474
17	6′-O-Acetylglycitin	10228095	488.4	134859-96-4	CHEBI:133348
18	13-Deoxy-Isogibberellic acid	51136328	330.4	–	–
19	Daucoidin A	6479092	344.4	103629-87-4	–
20	3,5-Diprenyl-4-hydroxybenzaldehyde	71519781	258.35	52275-04-4	–
21	Sucrose	5988	342.3	57-50-1	CHEBI:17992

corresponding to functional loop dynamics. Comparable Rg (1.55–1.58 nm) and SASA (78–83 nm²) with the apo protein confirmed preserved tertiary structure integrity. A stable hydrogen-bonding network (1–2 persistent H-bonds) further supported dynamic equilibrium at the binding interface. This IL-1β complex (Figure 8B) demonstrated greater conformational plasticity, with RMSD (3.5–4.5 Å) significantly higher than unbound IL-1β (2.0–3.0 Å), yet maintaining controlled fluctuations (<10% deviation). The complex exhibited RMSF fluctuations similar to unbound IL-1β, with the majority of residues displaying modest fluctuations (0.5–2.5 Å), indicating well-maintained global backbone stability. The prominent RMSF peak (4.5–5.0 Å) at residues 50–60 suggested localized flexibility enhancement, while subtle increases in Rg (1.57–1.60 nm vs 1.53–1.56 nm) and SASA (90–98 nm² vs 85–93 nm²) reflected moderate structural expansion. The hydrogen-bonding pattern (1–2 primary H-bonds) mirrored that of the TNF complex, demonstrating analogous binding stability. Thus, MD simulation results confirm the stable binding of the TNF-21-deoxyneridienone B and IL-1β-13-Deoxy-Isogibberellic acid complexes, demonstrating high consistency with the molecular docking predictions. These findings further confirm that the ligand-induced stabilization of target protein conformations is a crucial molecular mechanism by which DS regulates inflammatory targets in adenomyosis.

DS Effectively Ameliorated the Pathological Changes Associated with Adenomyosis

A detailed flowchart of the in vivo assays is presented in Figure 9A. H&E staining results indicated that compared to the control group, the adenomyosis model group exhibited disordered endometrial architecture with glandular and stromal cell invasion into the myometrium. Intervention with Gestrinone and DS effectively ameliorated the structural disorganization of the endometrium to varying extents, with the therapeutic effects of DS demonstrating a dose-dependent manner (Figure 9B).

Validation of Key Targets in Signaling Pathways Using qRT-PCR, WB, and IF Methods

The core targets within the TNF-α, IL-17, and HIF-1 signaling pathways include TNF-α, IL-17A, IL-1β, and HIF-1α. qRT-PCR and WB analyses demonstrated that the expression levels of TNF-α, IL-17A, IL-1β, and HIF-1α at the mRNA

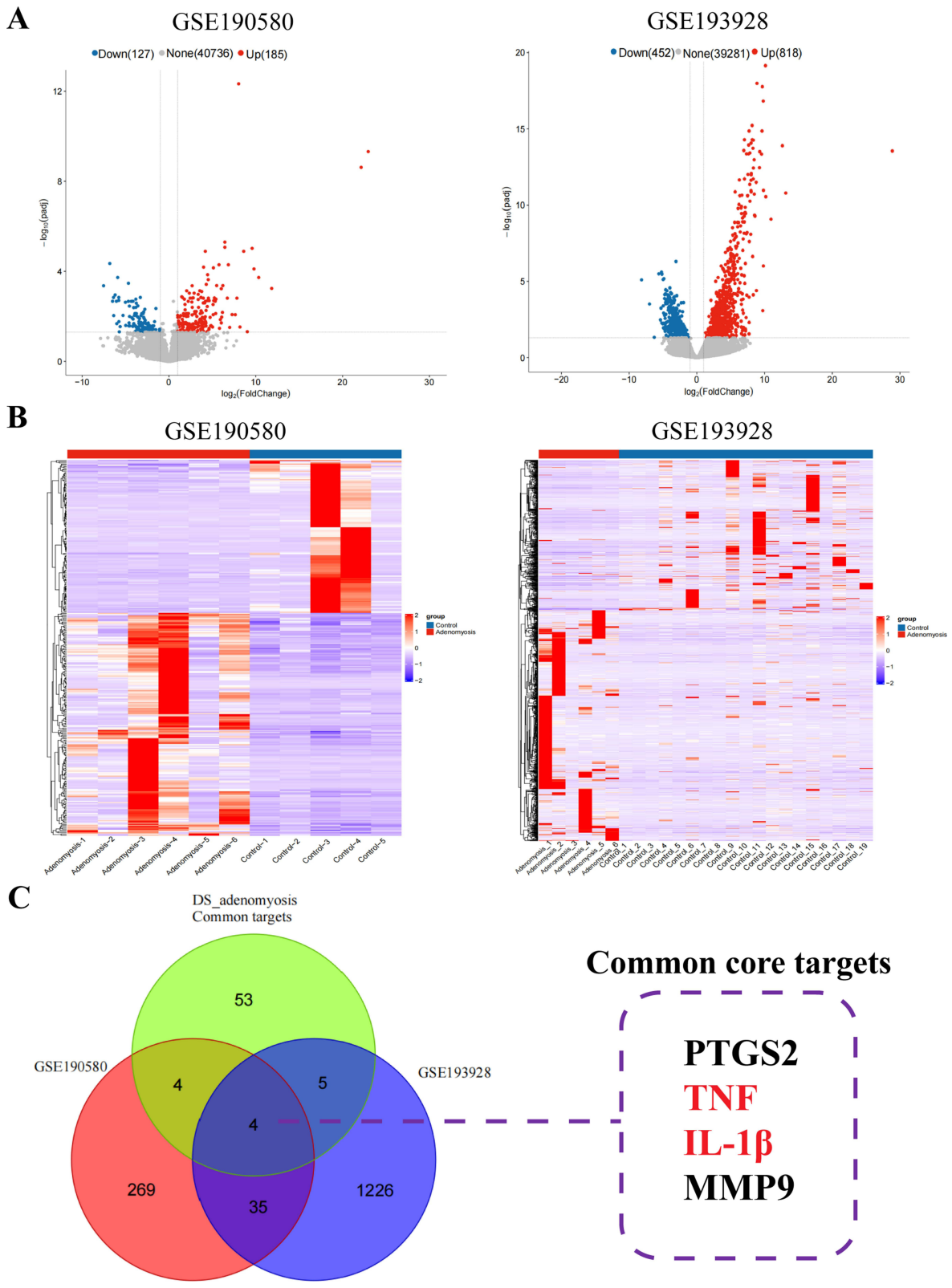

Figure 7 Validation of core targets for DS in treating adenomyosis from GEO datasets. (**A**) Volcano plot illustrating differentially expressed genes. (**B**) Hierarchical clustering heatmap of the DEGs. (**C**) Venn diagram demonstrating the intersection between DS-adenomyosis targets and DEG datasets. Red font highlights IL-1β and TNF as hub node that coregulate the TNF/IL-17/HIF-1α signaling pathways in subsequent studies.

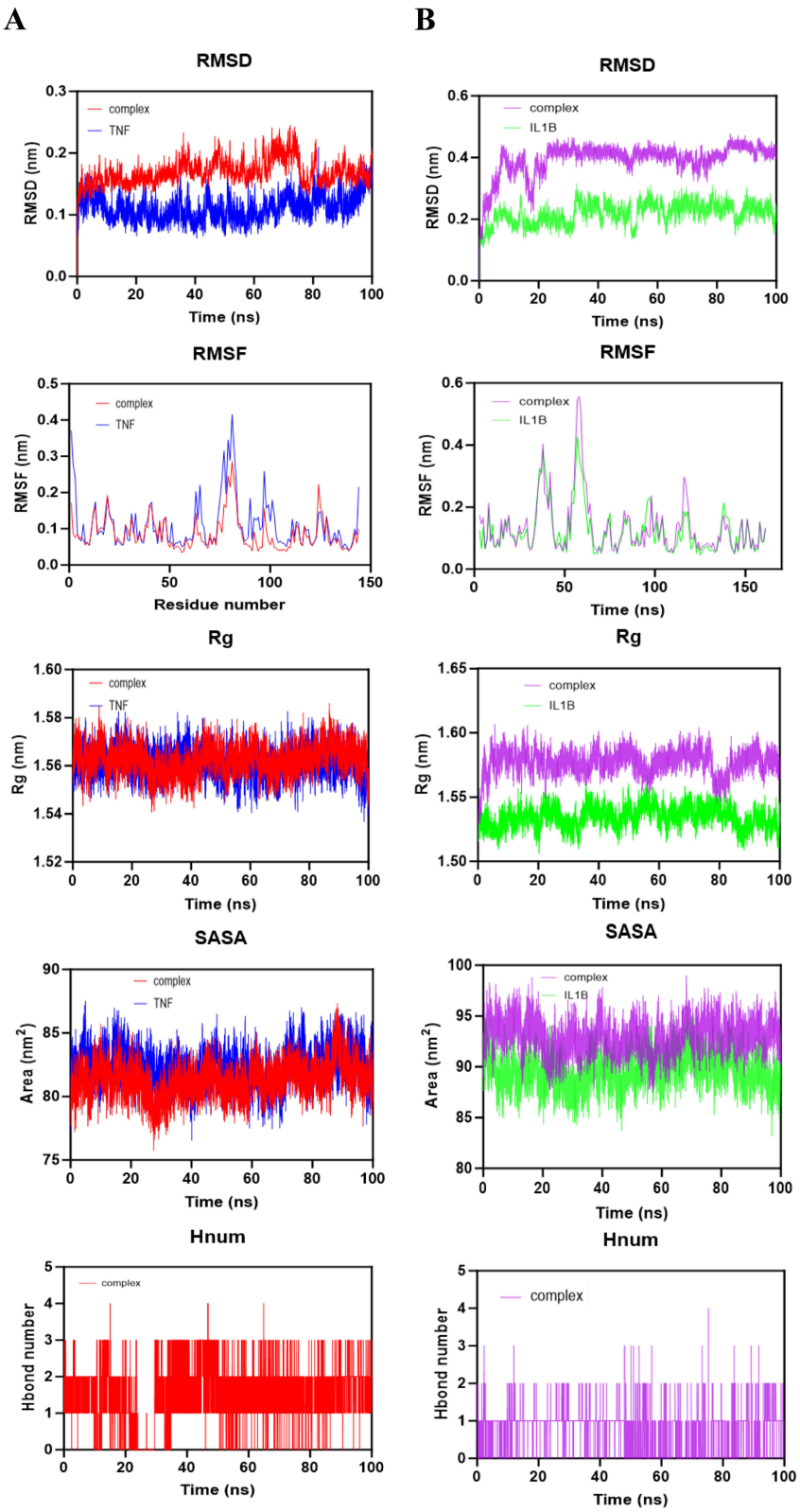

Figure 8 Molecular dynamics simulations of bioactive compounds and target proteins. (**A**) TNF and 21-Deoxyneridienone B. (**B**) IL-1β and 13-Deoxy-Isogibberellic.

https://doi.org/10.2147/JIR.S537221

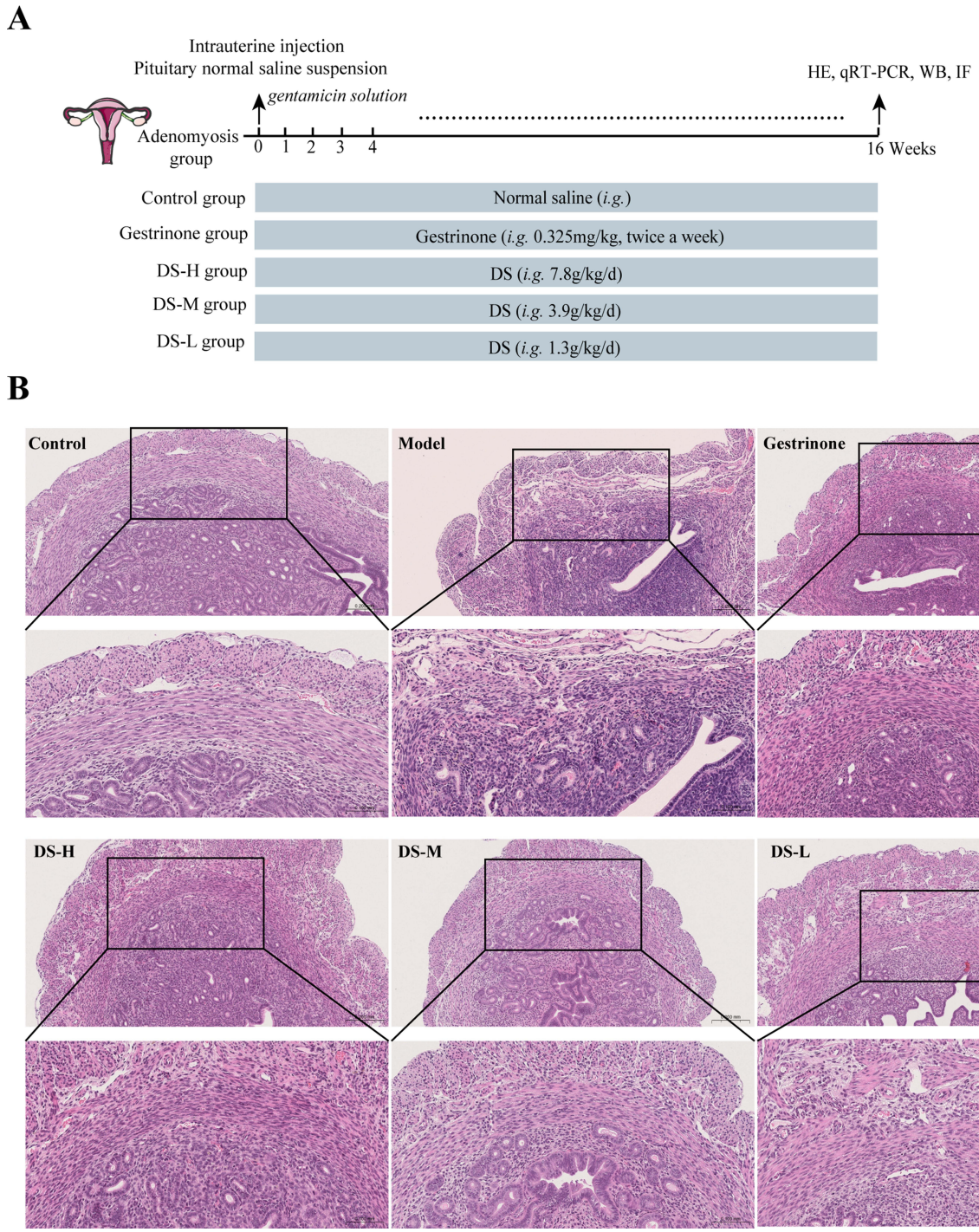

Figure 9 DS effectively ameliorated the pathological changes associated with adenomyosis. (**A**) The diagram of animal experiments. (**B**) H&E staining of Control, Model, Gestrinone, DS-H, DS-M, and DS-L (Scale bar: 100 μM and 200 μM, n = 3).

and protein levels were significantly elevated in the adenomyosis model group. Treatment with DS resulted in a concentration-dependent reduction in the expression of these targets (Figure 10A, B and Supplementary Figure 1). IF analysis of TNF-α and IL-17A expression (Figure 10C) further validated these findings, illustrating that DS ameliorates adenomyosis, which aligns with the outcomes observed in qRT-PCR and WB analyses. These findings suggest that DS effectively mitigates adenomyosis through modulation of the TNF-α, IL-17, and HIF-1 signaling pathways.

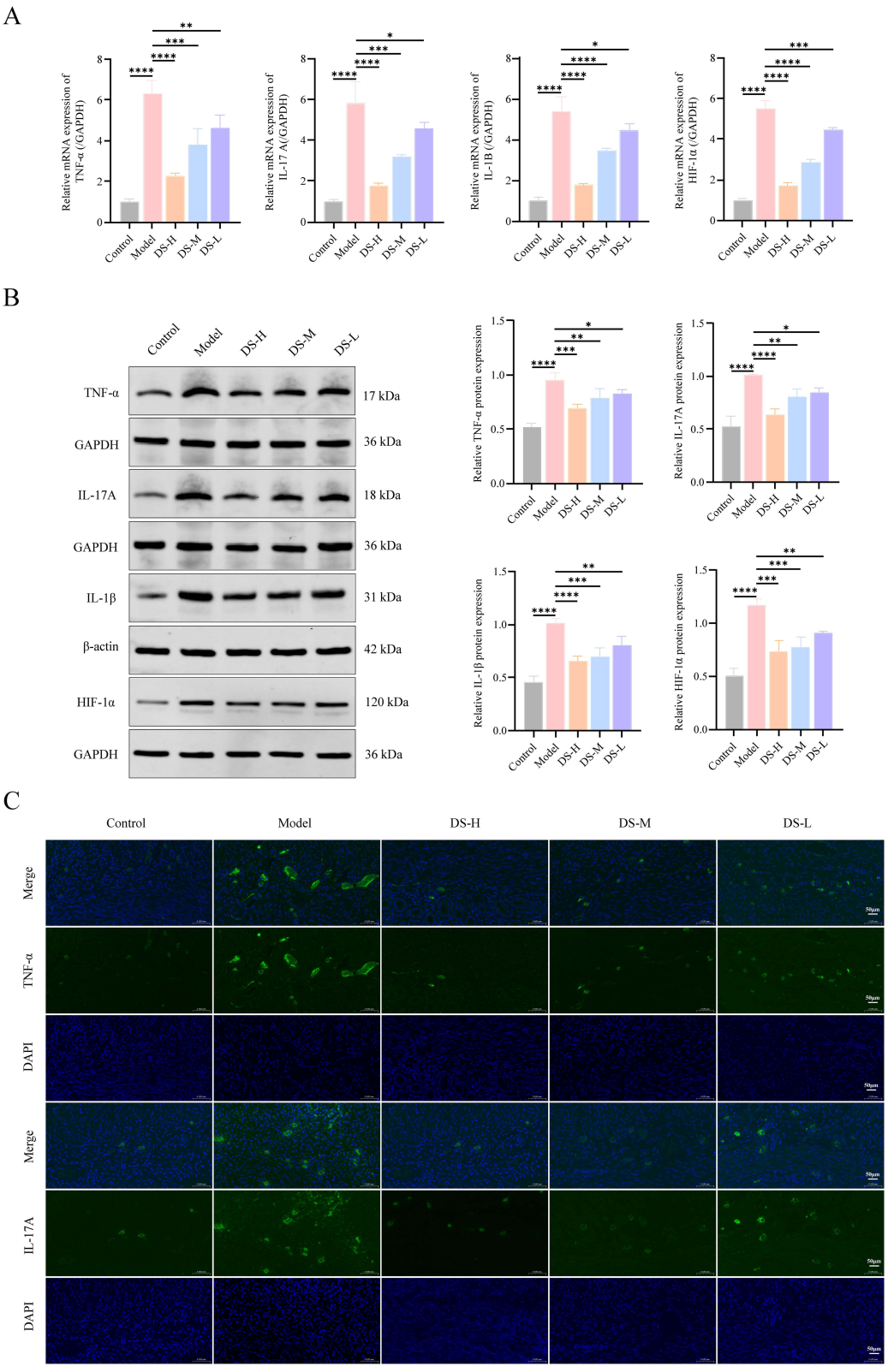

Figure 10 qRT-PCR, WB, and IF method verification for key targets in signaling pathways. (**A**) qRT-PCR of TNF-α, IL-17A, IL-1β, and HIF-1α mRNA expression. (**B**) Western Blot detection of TNF-α, IL-17A, IL-1β, and HIF-1α protein expression. (**C**) Immunofluorescence staining shows the fluorescent expression of TNF-α and IL-17A (Scale bar: 50 μM, n = 3). Data were expressed as mean ± SD (n = 3) *p<0.05, **p<0.01, ***p<0.001, ****p<0.0001 VS Model.

https://doi.org/10.2147/JIR.S537221

Discussion

This study aimed to preliminarily investigate the potential active components of DS and their mechanisms of action against adenomyosis by integrating various pharmacology methodologies with experiment confirmed. The UPLC-QE-MS identified 35 potential bioactive from IAIBs of DS. Network pharmacology predicted that DS might exert its therapeutic effects on adenomyosis by modulating TNF-α, IL-17, and HIF-1α signaling pathways associated with inflammation. Molecular docking results demonstrated that the active components have strong affinities with core targets including *TNF, IL1β, MMP2, ESR1, PTGS2, STAT3, BCL2, AKT1, MMP9, and EGFR*. Transcriptomic validation identified *TNF* and *IL-1β* as key therapeutic targets, which was further corroborated by MD simulations demonstrating stable binding conformations between DS bioactive compounds and these pivotal inflammatory targets. In Vivo studies confirmed that DS may exert therapeutic effects against adenomyosis by modulating TNF-α, IL-17, and HIF-1α singing pathways of inflammatory, consistent with network pharmacology predictions. These findings offer compelling evidence of DS's therapeutic potential in modulating the inflammatory pathogenesis and support DS as a promising candidate for adenomyosis.

Adenomyosis is a chronic inflammatory disorder characterized by dysregulated cytokine expression with activating inflammatory pathways, particularly the overproduction of pro-inflammatory mediators (eg, TNF, IL-1β, IL-17) and impaired anti-inflammatory responses in adenomyotic lesions.[39–41,44] These imbalances sustain a pathological micro-environment that promotes ectopic endometrial invasion and disease progression.[45] Current hormonal therapies remain limited by side effects and high recurrence rates,[46] necessitating safer alternatives targeting inflammatory pathways. Furthermore, our transcriptomic profiling confirm dysregulated IL-1β and TNF expression patterns in adenomyotic ectopic lesions, establishing these inflammatory mediators as mechanistically grounded therapeutic targets. This aligns with the "multi-component, multi-target, and multi-pathway" paradigm of TCM, which has shown efficacy in complex gynecological diseases.[47] Specifically, DS is a widely used TCM for multiple diseases, which exerts pleiotropic effects by coordinately modulating inflammation, coagulation, and fibrosis.[48] Its clinical benefits for adenomyosis may stem from anti-inflammatory effects in multiple organs, including selective downregulation of key cytokines (IL-1β and TNF-α),[49,50] modulation of TNF-α/IL-17/HIF-1α pathways,[51,52] and synergistic actions across multiple pathological axes.[53] This multi-target engagement profile of anti-inflammatory pathways provides a mechanistic basis for DS's anti-adenomyosis effects, distinguishing it from single-target hormonal therapies. Further investigation of critical inflammatory pathways may provide deeper insights into DS's efficacy and applications for adenomyosis.

Our network pharmacology and KEGG enrichment analysis identifies the TNF-α and IL-17 signaling pathways as primary inflammatory pathways of DS-adenomyosis. These pathways are pivotal in adenomyosis-associated inflammation, where aberrant TNF and IL-17 expression recruits immune cells, amplifies inflammatory cascades, and exacerbates tissue damage.[44] By suppressing these pathways, DS may restore cytokine equilibrium, attenuate lesion inflammation, and impede disease advancement. This mechanistic rationale is supported by DS's ability to alleviate dysmenorrhea[54] and pelvic inflammation,[55] offering a theoretical foundation for its repurposing in adenomyosis therapy. Furthermore, DS's therapeutic potential extends to mitigating hypoxia-driven pathology via the HIF-1α signaling pathway.[56] Adenomyosis lesions often exhibit hypoxic and oxidative stress conditions, which activate HIF-1 to promote angiogenesis, metabolic reprogramming, and neuroinflammation-processes linked to pain and disease aggravation.[57,58] DS's putative inhibition of HIF-1 could disrupt this vicious cycle, reducing hypoxia-induced tissue damage and inflammatory responses.[59] Together, these findings position DS as a promising candidate for adenomyosis treatment, leveraging its multi-pathway anti-inflammatory actions to address both symptoms and underlying pathogenesis. Future research should validate these targets experimentally and explore DS's synergies with conventional therapies to optimize clinical outcomes.

Additionally, an integrated computational analysis including molecular docking and MD simulations were used to evaluate drug-target stability to validate bioactive compound screening.[43] This state-of-the-art computational framework provides a technological platform for exploiting the drug repurposing potential of phytochemical constituents.[60] Our quantitative assessment revealed that DS-derived phytochemicals exhibited potent binding interactions with key inflammatory mediators of TNF-α and IL-1β, achieving a mean binding energy of −8 kcal/mol. This significantly exceeds the established thresholds for biological activity (−5.0 kcal/mol) and strong binding affinity (−7.0 kcal/mol).[61] MD

simulations are a powerful computational tool for investigating protein interactions with drug-like small molecules at atomic resolution.[62] They have become indispensable in modern drug design, playing a pivotal role in elucidating the dynamic behavior and conformational changes of protein-ligand complexes at atomic resolution.[63] Through 100-ns MD simulations, we observed a mild increase in the RMSD of the TNF-21-Deoxyneridienone B complex (1.5–2.0 Å) compared to unliganded TNF (1.0–1.5 Å), yet it remained significantly below 2 Å. Importantly, the complex maintained a notably low mean RMSF, indicating that this controlled enhancement of structural flexibility might facilitate signal transduction while preserving the overall structural integrity of the protein-ligand complex. These results are consistent with the stability data by reported McMillan et al[64] for TNF-α/small-molecule complexes. In contrast, the IL-1β-13-Deoxy-Isogibberellic acid complex exhibited higher RMSD values (3.5–4.5 Å) compared to unbound IL-1β (2.0–3.0 Å) while maintaining fluctuations within 10% of the mean. Notably, the average RMSF (1.34 Å) for the complex remained predominantly below 2 Å, suggesting a well-maintained structural framework despite increased global flexibility, aligning with previous studies.[65] These results confirmed that DS active compounds directly binds to TNF and IL1β to regulate inflammation and anti-adenomyosis. This comprehensive computational validation not only elucidates the therapeutic mechanisms of DS at the atomic level but also establishes a theoretical framework for developing multi-target anti-inflammatory therapies for adenomyosis.

In summary, inflammation plays a crucial role in the pathogenesis of adenomyosis,[66] characterized by chronic inflammatory responses that trigger local immune cell activation and sustained release of inflammatory mediators.[39,67–69] Proinflammatory cytokines such as TNF-α, IL-1β, IL-6, and IL-17 promote the proliferation and migration of endometrial cells, contributing to adenomyosis progression.[39,70] Additionally, inflammation-induced angiogenesis provides nutritional support for ectopic lesions, exacerbating disease advancement.[71] Using an established adenomyosis mouse model, we demonstrated that DS can restore endometrial tissue architecture and significantly reduce glandular-stromal invasion into the myometrium, as demonstrated by H&E staining. Further molecular analyses, including qRT-PCR, WB, and IF, confirmed that DS mediates the downregulation of TNF-α, IL1β, IL-17, and HIF-1α expression at both transcriptional and translational levels showing statistical significance. These findings suggest that DS exerts therapeutic effects of anti-inflammatory through coordinated modulation of TNF-α/IL-17/HIF-1α signaling pathways, transcending the limitations of single-target drugs. The observed efficacy arises from DS's unique polypharmacological capacity to simultaneously regulate multiple signaling cascades and molecular targets, resulting in synergistic therapeutic outcomes.[72] Our study provides compelling evidence that DS ameliorates adenomyosis by targeting TNF-α/IL-17/HIF-1α singing pathways, thereby establishing a solid foundation for the clinical translation and development of novel multi-target therapeutics for adenomyosis.

The multi-component and multi-target nature of TCM offers therapeutic advantages for DS-adenomyosis but also poses challenges due to inherent variability in bioactivity and mechanisms. Consequently, the current study has limitations. First, research on how these compounds collectively contribute to the treatment of adenomyosis remains insufficiently explored, particularly regarding the mechanisms of action of key bioactive components in DS and the specific details of their synergistic effects, which require further investigation. Second, only representative molecules from key biological functional modules were selected for analysis in the molecular validation experiments. This selection may limit a comprehensive and in-depth understanding of the mechanistic actions of DS. Future studies should focus on the monomeric compounds of DS identified validate this study's findings, employing gene knockout rats and rescue experiments targeting potential pathways to strengthen the evidence base. Additionally, while our target screening covered major genetic and pharmacological databases, the rapidly evolving nature of disease-gene annotations warrants periodic updates. Future studies could incorporate emerging resources like Open Targets when more adenomyosis data become available. Although the safety and stability of DS, a plant-based TCM with a long history, have been established, well-designed clinical studies are essential. This includes randomized controlled trials with standardized protocols and rigorous outcome assessments to validate the therapeutic efficacy and safety of DS in managing adenomyosis. While our study demonstrates DS's therapeutic potential in adenomyosis through modulation of TNF-α/IL-17/HIF-1α signaling pathways, certain limitations should be acknowledged. The current findings, primarily derived from animal models and bioinformatics analyses, would benefit from: (1) mechanistic validation using genetic perturbations (eg, knockout/knockin) or pharmacological interventions; (2) in vitro confirmation of its dual regulatory (agonist/antagonist) effects; and (3) translational studies including dose-response assessments, PK/PD analyses,

and validation in patient-derived models (eg, organoids/xenografts) to strengthen clinical relevance. These aspects will be prioritized in future investigations.

Conclusions

This study systematically elucidates the multi-target synergistic mechanisms of DS bioactive compounds against adenomyosis using an integrated approach that combines pharmacologic, transcriptomic, and in vivo analyses. These findings suggest that DS exerts its therapeutic effects on adenomyosis by modulating inflammatory factors through multiple pathways and targets, including the TNF-α, IL-17, and HIF-1α signaling pathways. This study indicates that DS is a promising option within TCM for treating adenomyosis. Our elucidation of the specific molecular mechanism of DS anti-adenomyosis and its effective active ingredients provide a theoretical foundation for enhancing the clinical application of TCM, thereby supporting future clinical research and drug development.

Data Sharing Statement

Data is contained within the article or Supplementary Materials, and reasonable inquiries can be available from the corresponding author Junying Jiang. Existing datasets are available in a publicly accessible repository: Publicly available datasets were analyzed in this study. This data can be found from the GEO database (https://www.ncbi.nlm.nih.gov/geo/): GSE193928 and GSE190580.

Ethics Statement

All animal experiments were approved by the Experimental Animal Ethics Committee of Fujian Medical University (approval code: IACUC-FJMU-2023-Y-0804) and conducted in compliance with the Guidelines for Ethical Review of Welfare of Chinese Experimental Animals (GB/T 35892-2018). The human data analyzed in this study were obtained from publicly available online databases. According to Items 1 and 2 of Article 32 of China's Measures for Ethical Review of Life Science and Medical Research Involving Human Subjects (effective February 18, 2023), this study qualifies for exemption from additional institutional ethical review.

Funding

The author(s) declare that financial support was received for this article's research, authorship, and/or publication. This study was supported by the Fujian Provincial Natural Science Foundation of China (Grant NO.2023J011216); Joint Funds for the Innovation of Science and Technology of Fujian Province (Grant NO.2023Y9391); Fujian Provincial Health Technology Project (Grant NO.2023CXA039).

Disclosure

The authors report no conflicts of interest in this work.

References

1. Kobayashi H. Molecular targets for nonhormonal treatment based on a multistep process of adenomyosis development. *Reprod Sci*. 2023;30(3):743–760. doi:10.1007/s43032-022-01036-4
2. Vannuccini S, Petraglia F. Recent advances in understanding and managing adenomyosis. *F1000Res*. 2019;8:283. doi:10.12688/f1000research.17242.1
3. Donnez J, Stratopoulou CA, Dolmans MM. Endometriosis and adenomyosis: similarities and differences. *Best Pract Res Clin Obstet Gynaecol*. 2024;92:102432. doi:10.1016/j.bpobgyn.2023.102432
4. Rees CO, van Vliet H, Siebers A, et al. The ADENO study: aDenomyosis and its effect on neonatal and obstetric outcomes: a retrospective population-based study. *Am J Obstet Gynecol*. 2023;229(1):49e1–49e12. doi:10.1016/j.ajog.2022.12.013
5. Xu W, Song Y, Li K, Zhang B, Zhu X. Quercetin inhibits adenomyosis by attenuating cell proliferation, migration and invasion of ectopic endometrial stromal cells. *Drug Des Devel Ther*. 2020;14:3815–3826. doi:10.2147/DDDT.S265066
6. Younes G, Tulandi T. Conservative surgery for adenomyosis and results: a systematic review. *J Minim Invasive Gynecol*. 2018;25(2):265–276. doi:10.1016/j.jmig.2017.07.014
7. Chao X, Song X, Wu H, You Y, Li L, Lang J. Adjuvant therapy in conservative surgery for adenomyosis. *Int J Gynaecol Obstet*. 2021;154(1):119–126. doi:10.1002/ijgo.13573
8. Xu Y, Shao L, Zhou Z, et al. ARG2 knockdown promotes G0/G1 cell cycle arrest and mitochondrial dysfunction in adenomyosis via regulation NF-κB and Wnt/B-catenin signaling cascades. *Int Immunopharmacol*. 2024;140:112817. doi:10.1016/j.intimp.2024.112817

9. Shen F, Liu Y, Lin L, Zhao M, Chen Q. Association of benign gynaecological diseases and risk of endometrial and ovarian cancers. *J Cancer*. 2020;11(11):3186–3191. doi:10.7150/jca.39626
10. Inoue S, Hirota Y, Ueno T, et al. Uterine adenomyosis is an oligoclonal disorder associated with KRAS mutations. *Nat Commun*. 2019;10(1):5785. doi:10.1038/s41467-019-13708-y
11. Vannuccini S, Luisi S, Tosti C, Sorbi F, Petraglia F. Role of medical therapy in the management of uterine adenomyosis. *Fertil Steril*. 2018;109(3):398–405. doi:10.1016/j.fertnstert.2018.01.013
12. Latif S, Kastora S, Al Wattar BH, Yasmin E, Saridogan E, Mavrelos D. The effectiveness of prolonged downregulation with gonadotrophin-releasing hormone analogue (GnRHa) treatment in women with adenomyosis undergoing IVF/ICSI: a systematic review and meta-analysis. *Eur J Obstet Gynecol Reprod Biol*. 2024;301:87–94. doi:10.1016/j.ejogrb.2024.07.063
13. Wang J, Wong YK, Liao F. What has traditional Chinese medicine delivered for modern medicine? *Expert Rev Mol Med*. 2018;20:e4. doi:10.1017/erm.2018.3
14. Huang L, Ji X, Wang X, et al. Adjuvant therapy of Chinese herbal medicine for the treatment of adenomyosis: a protocol for systematic review. *Medicine*. 2020;99(25):e20560. doi:10.1097/MD.0000000000020560
15. Ying P, Li H, Jiang Y, et al. Qiu's Neiyi recipe regulates the inflammatory action of adenomyosis in mice via the MAPK signaling pathway. *Evid Based Complement Alternat Med*. 2021;2021:9791498. doi:10.1155/2021/9791498
16. Feng T, Wei S, Wang Y, et al. Rhein ameliorates adenomyosis by inhibiting NF-kappaB and beta-Catenin signaling pathway. *Biomed Pharmacother*. 2017;94:231–237. doi:10.1016/j.biopha.2017.07.089
17. Khan KN, Kitajima M, Inoue T, et al. Additive effects of inflammation and stress reaction on Toll-like receptor 4-mediated growth of endometriotic stromal cells. *Hum Reprod*. 2013;28(10):2794–2803. doi:10.1093/humrep/det280
18. Liu M, Li Z, Ouyang Y, et al. Material basis and integrative pharmacology of danshen decoction in the treatment of cardiovascular diseases. *Phytomedicine*. 2023;108:154503. doi:10.1016/j.phymed.2022.154503
19. Zhou ZH, Weng Q, Zhou JH, Zhou J. Extracts of Salvia miltiorrhiza Bunge on the cytokines of rat endometriosis models. *Afr J Tradit Complement Altern Med*. 2012;9(3):303–314. doi:10.4314/ajtcam.v9i3.2
20. Jin Z, Chenghao Y, Cheng P. Anticancer effect of tanshinones on female breast cancer and gynecological cancer. *Front Pharmacol*. 2021;12:824531. doi:10.3389/fphar.2021.824531
21. Xu X, Zhang Z, Liu L, Che C, Li W. Exploring the antiovarian cancer mechanisms of salvia miltiorrhiza bunge by network pharmacological analysis and molecular docking. *Comput Math Methods Med*. 2022;2022:7895246. doi:10.1155/2022/7895246
22. Shen W, Zhang Y, Li W, et al. Effects of tanshinone on hyperandrogenism and the quality of life in women with polycystic ovary syndrome: protocol of a double-blind, placebo-controlled, randomised trial. *BMJ Open*. 2013;3(10):e003646. doi:10.1136/bmjopen-2013-003646
23. Zhang X, Lin L, Li H, et al. Update on new trend and progress of the mechanism of polysaccharides in the intervention of Alzheimer's disease, based on the new understanding of relevant theories: a review. *Int J Biol Macromol*. 2022;218:720–738. doi:10.1016/j.ijbiomac.2022.07.158
24. Zhao X, Su H, Chen H, et al. Integrated serum pharmacochemistry and network pharmacology to explore the mechanism of Yi-Shan-Hong formula in alleviating chronic liver injury. *Phytomedicine*. 2024;128:155439. doi:10.1016/j.phymed.2024.155439
25. Lv J, Qin M, Pang X, et al. Molecular mechanism of regulating tat protein expression of pingganjiedu TCM in the treatment of AIDS based on network pharmacology. *Int J Biol Macromol*. 2024;278(Pt 1):134599. doi:10.1016/j.ijbiomac.2024.134599
26. Zhao L, Zhang H, Li N, et al. Network pharmacology, a promising approach to reveal the pharmacology mechanism of Chinese medicine formula. *J Ethnopharmacol*. 2023;309:116306. doi:10.1016/j.jep.2023.116306
27. Shan X, Li J, Hong B, et al. Comparative efficacy of sweated and non-sweated Salvia miltiorrhiza Bge. extracts on acute myocardial ischemia via regulating the PPARalpha/RXRalpha/NF-kappaB signaling pathway. *Heliyon*. 2024;10(11):e31923. doi:10.1016/j.heliyon.2024.e31923
28. Pan W, Jin M, Cui Z, Liu X, Wang M, Piu C. Clinical application and dosage investigation of Salvia miltiorrhiza (Danshen). *Jilin J Trad Chin Med*. 2019;39(06):722–725.
29. Ai ZL, Zhang X, Ge W, et al. Salvia miltiorrhiza extract may exert an anti-obesity effect in rats with high-fat diet-induced obesity by modulating gut microbiome and lipid metabolism. *World J Gastroenterol*. 2022;28(43):6131–6156. doi:10.3748/wjg.v28.i43.6131
30. Nwafor EO, Lu P, Li J, et al. Traditional Chinese medicine of Salvia miltiorrhiza Bunge: a review of phytochemistry, pharmacology and pharmacokinetics. *Trad Med Res*. 2021;6:35. doi:10.53388/TMR20201027204
31. Shen YZ, Yao YD, Li HL, Li Y, Hu YC. CTSO and HLA-DQA1 as biomarkers in sepsis-associated ARDS: insights from RNA sequencing and immune infiltration analysis. *BMC Infect Dis*. 2025;25(1):326. doi:10.1186/s12879-025-10726-8
32. Mu H, Chen J, Huang W, et al. OmicShare tools: a zero-code interactive online platform for biological data analysis and visualization. *Imeta*. 2024;3(5):e228. doi:10.1002/imt2.228
33. Trott O, Olson AJ. AutoDock Vina: improving the speed and accuracy of docking with a new scoring function, efficient optimization, and multithreading. *J Comput Chem*. 2010;31(2):455–461. doi:10.1002/jcc.21334
34. Zhu N, Hou J. Exploring the mechanism of action Xianlingubao Prescription in the treatment of osteoporosis by network pharmacology. *Comput Biol Chem*. 2020;85:107240. doi:10.1016/j.compbiolchem.2020.107240
35. Peluso P, Chankvetadze B. Recent developments in molecular modeling tools and applications related to pharmaceutical and biomedical research. *J Pharm Biomed Anal*. 2024;238:115836. doi:10.1016/j.jpba.2023.115836
36. Yu X, Qin W, Cai H, et al. Analyzing the molecular mechanism of xuefuzhuyu decoction in the treatment of pulmonary hypertension with network pharmacology and bioinformatics and verifying molecular docking. *Comput Biol Med*. 2024;169:107863. doi:10.1016/j.compbiomed.2023.107863
37. Ullah A, Sun Q, Li J, et al. Bioactive compounds in Citrus reticulata peel are potential candidates for alleviating physical fatigue through a triad approach of network pharmacology, molecular docking, and molecular dynamics modeling. *Nutrients*. 2024;16(12):1934. doi:10.3390/nu16121934
38. Xie YQ, Yan FN, Yu LH, Yan HW, Kong YX, Yang ZY. Mechanism of Shashen-Maidong herb pair in treating hepatocellular carcinoma using network pharmacology and experimental validation. *J Ethnopharmacol*. 2025;337(Pt 3):118954. doi:10.1016/j.jep.2024.118954
39. Bourdon M, Santulli P, Jeljeli M, et al. Immunological changes associated with adenomyosis: a systematic review. *Hum Reprod Update*. 2021;27(1):108–129. doi:10.1093/humupd/dmaa038
40. Carrarelli P, Yen CF, Funghi L, et al. Expression of inflammatory and neurogenic mediators in adenomyosis. *Reprod Sci*. 2017;24(3):369–375. doi:10.1177/1933719116657192
41. Bulun SE, Yilmaz BD, Sison C, et al. Endometriosis. *Endocr Rev*. 2019;40(4):1048–1079. doi:10.1210/er.2018-00242

42. Chi Z, Wei G, Ling-Ling S, Han-Rui C, Li-Zhu L. Network pharmacology-based analysis of the mechanism of action of the Herb Pair Chai Hu - Bai Shao. *Digital Chin Med*. 2019;2(4):227–236. doi:10.1016/j.dcmed.2020.01.004
43. Zhang Y, Zhang D, Li M, et al. Molecular docking and dynamics of a dextranase derived from Penicillium cyclopium CICC-4022. *Int J Biol Macromol*. 2023;253(Pt 2):126493. doi:10.1016/j.ijbiomac.2023.126493
44. Shi JL, Zheng ZM, Chen M, Shen HH, Li MQ, Shao J. IL-17: an important pathogenic factor in endometriosis. *Int J Med Sci*. 2022;19(4):769–778. doi:10.7150/ijms.71972
45. Guo SW. The Pathogenesis of Adenomyosis vis-a-vis Endometriosis. *J Clin Med*. 2020;9(2):485. doi:10.3390/jcm9020485
46. Khan KN, Fujishita A, Mori T. Pathogenesis of human adenomyosis: current understanding and its association with infertility. *J Clin Med*. 2022;11 (14):4057. doi:10.3390/jcm11144057
47. Yang H, Lee YH, Lee SR, Kaya P, Hong EJ, Lee HW. Traditional medicine (Mahuang-Tang) improves ovarian dysfunction and the regulation of steroidogenic genes in Letrozole-induced PCOS Rats. *J Ethnopharmacol*. 2020;248:112300. doi:10.1016/j.jep.2019.112300
48. Jung I, Kim H, Moon S, Lee H, Kim B. Overview of Salvia miltiorrhiza as a potential therapeutic agent for various diseases: an update on efficacy and mechanisms of action. *Antioxidants*. 2020;9(9).
49. Zou LF, Liu DF, Yang H, et al. Salvianolic acids from Salvia miltiorrhiza Bunge and their anti-inflammatory effects through the activation of α7nAchR signaling. *J Ethnopharmacol*. 2023;317:116743. doi:10.1016/j.jep.2023.116743
50. Ye T, Li Y, Xiong D, et al. Combination of Danshen and ligustrazine has dual anti-inflammatory effect on macrophages and endothelial cells. *J Ethnopharmacol*. 2021;266:113425. doi:10.1016/j.jep.2020.113425
51. Chen G, Jin Z, Wang X, Yu QH, Hu GB. Danshen injection mitigated the cerebral ischemia/reperfusion injury by suppressing neuroinflammation via the HIF-1α/CXCR4/NF-κB signaling pathway. *Neuroreport*. 2024;35(10):601–611. doi:10.1097/WNR.0000000000002043
52. Ye X, Liu J, Yuan X, Yang S, Huang Y, Chen Y. Molecular mechanism of Salvia miltiorrhiza bunge in treating cerebral infarction. *Evid Based Complement Alternat Med*. 2022;2022:5992394. doi:10.1155/2022/5992394
53. Guo R, Li L, Su J, et al. Pharmacological activity and mechanism of tanshinone IIA in related diseases. *Drug Des Devel Ther*. 2020;14:4735–4748. doi:10.2147/DDDT.S266911
54. Su CC, Chen GW, Lin JG. Growth inhibition and apoptosis induction by tanshinone I in human colon cancer Colo 205 cells. *Int J Mol Med*. 2008;22(5):613–618.
55. Zou W, Gong L, Zhou F, et al. Anti-inflammatory effect of traditional Chinese medicine preparation Penyanling on pelvic inflammatory disease. *J Ethnopharmacol*. 2021;266:113405. doi:10.1016/j.jep.2020.113405
56. Chen Q, Liu Y, Zhu Y, et al. Cryptotanshinone inhibits PFK-mediated aerobic glycolysis by activating AMPK pathway leading to blockade of cutaneous melanoma. *Chin Med*. 2024;19(1):45. doi:10.1186/s13020-024-00913-1
57. Dai W, Guo R, Na X, et al. Hypoxia and the endometrium: an indispensable role for HIF-1alpha as therapeutic strategies. *Redox Biol*. 2024;73:103205. doi:10.1016/j.redox.2024.103205
58. Guo S, Zhang D, Lu X, et al. Hypoxia and its possible relationship with endometrial receptivity in adenomyosis: a preliminary study. *Reprod Biol Endocrinol*. 2021;19(1):7. doi:10.1186/s12958-020-00692-y
59. Li X, Liu R, Liu W, et al. Panax quinquefolium L. and Salvia miltiorrhiza bunge. Enhances angiogenesis by regulating the miR-155-5p/HIF-1α/VEGF axis in acute myocardial infarction. *Drug Des Devel Ther*. 2023;17:3249–3267. doi:10.2147/DDDT.S426345
60. Yadav R, Baby K, Nayak Y, et al. Unveiling the potential of tankyrase I inhibitors for the treatment of type 2 diabetes mellitus: a hybrid approach using network pharmacology, 2D structural similarity, molecular docking, MD simulation and in-vitro studies. *Life Sci*. 2025;369:123548. doi:10.1016/j.lfs.2025.123548
61. Xu Y, Zhang J, Li X. Erjingwan and Alzheimer's disease: research based on network pharmacology and experimental confirmation. *Front Pharmacol*. 2024;15:1328334. doi:10.3389/fphar.2024.1328334
62. Jones D, Allen JE, Yang Y, et al. Accelerators for classical molecular dynamics simulations of biomolecules. *J Chem Theory Comput*. 2022;18 (7):4047–4069. doi:10.1021/acs.jctc.1c01214
63. Hu X, Zeng Z, Zhang J, Wu D, Li H, Geng F. Molecular dynamics simulation of the interaction of food proteins with small molecules. *Food Chem*. 2023;405(Pt A):134824. doi:10.1016/j.foodchem.2022.134824
64. McMillan D, Martinez-Fleites C, Porter J, et al. Structural insights into the disruption of TNF-TNFR1 signalling by small molecules stabilising a distorted TNF. *Nat Commun*. 2021;12(1):582. doi:10.1038/s41467-020-20828-3
65. Feng M, Luo F, Wu H, et al. Network pharmacology analysis and machine-learning models confirmed the ability of YiShen HuoXue decoction to alleviate renal fibrosis by inhibiting pyroptosis. *Drug Des Devel Ther*. 2023;17:3169–3192. doi:10.2147/DDDT.S420135
66. Zhang H, Li C, Li W, Xin W, Qin T. Research advances in adenomyosis-related signaling pathways and promising targets. *Biomolecules*. 2024;14 (11):1402. doi:10.3390/biom14111402
67. Maclean A, Barzilova V, Patel S, Bates F, Hapangama DK. Characterising the immune cell phenotype of ectopic adenomyosis lesions compared with eutopic endometrium: a systematic review. *J Reprod Immunol*. 2023;157:103925. doi:10.1016/j.jri.2023.103925
68. Bourdon M, Santulli P, Doridot L, et al. Immune cells and Notch1 signaling appear to drive the epithelial to mesenchymal transition in the development of adenomyosis in mice. *Mol Hum Reprod*. 2021;27(10). doi:10.1093/molehr/gaab053
69. Kobayashi H. Endometrial inflammation and impaired spontaneous decidualization: insights into the pathogenesis of adenomyosis. *Int J Environ Res Public Health*. 2023;20(4):3762. doi:10.3390/ijerph20043762
70. Du L, Du DH, Chen B, Ding Y, Zhang T, Xiao W. Anti-inflammatory activity of Sanjie Zhentong capsule assessed by network pharmacology analysis of adenomyosis treatment. *Drug Des Devel Ther*. 2020;14:697–713. doi:10.2147/DDDT.S228721
71. Harmsen MJ, Wong CFC, Mijatovic V, et al. Role of angiogenesis in adenomyosis-associated abnormal uterine bleeding and subfertility: a systematic review. *Hum Reprod Update*. 2019;25(5):647–671. doi:10.1093/humupd/dmz024
72. Cai X, Zhang H, Li T. Multi-target pharmacological mechanisms of Salvia miltiorrhiza against oral submucous fibrosis: a network pharmacology approach. *Arch Oral Biol*. 2021;126:105131. doi:10.1016/j.archoralbio.2021.105131